

Multiple parameter analysis for assessing and forecasting earthquake hazards in the Lake Van region, Turkey

Serkan Öztürk, Hamdi Alkan*

Öztürk, S., Alkan, H. 2023. Multiple parameter analysis for assessing and forecasting earthquake hazards in the Lake Van region, Turkey. *Baltica*, 36 (2), 133–154. Vilnius. ISSN 0067-3064.

Manuscript submitted 4 May 2023 / Accepted 23 November 2023 / Available online 11 December 2023

© Baltica 2023

Abstract. A detailed spatial-temporal analysis of the seismic activity in and around the Lake Van region was performed using several seismotectonic parameters such as b -value, Z -value, relative intensity (RI), pattern informatics (PI), and Coulomb stress changes. Correlations between these parameters were analyzed to estimate and forecast potential seismic hazards in the Lake Van region. Particular attention was paid to the parts of the study region that exhibited smaller b -values, higher Z -values, and high-stress changes at the beginning of 2022 and to the locations of earthquake hotspots determined from the composite earthquake forecast map for 2022–2032, i.e., Muradiye, Çaldıran, Özalp, Erçek, Van city center and Gevaş covering the faults of Çaldıran, Yeniköşk, Erciş, Malazgirt and the fault zones of Saray and Van. To provide more accurate interpretations regarding potential earthquake occurrences in the near future, the seismotectonic parameters analyzed in the scope of this study were compared with the corresponding seismological, geological, geodetical, and geochemical variables reported in the literature. This comparison showed that, firstly, our results are consistent with those reported in previous studies, and, secondly, all these variables should be interpreted in combination to correctly assess strong earthquake hazards. Furthermore, this type of multiple-parameter analysis may be important for the description of seismic, tectonic, and structural characteristics of the nature of the crust. Our findings show that almost all seismotectonic parameters indicative of anomaly regions, i.e., lower b -values, higher Z -values, high-stress distribution, and hotspots, were recorded in the same parts of the study region. Thus, the anomaly regions detected at the beginning of 2019 and between 2022 and 2032 may be considered to be potential zones of future great earthquakes. To summarize, the correlations among these variables may provide accurate information for assessing and forecasting earthquake hazards in this region.

Keywords: *Spatial-temporal evaluation; b-value; Z-value; Forecasting; Coulomb stress; Earthquake hazard*

✉ Serkan Öztürk* (serkanozturk@gumushane.edu.tr),  <https://orcid.org/0000-0003-1322-5164>

Hamdi Alkan (hamdialkan@yyu.edu.tr),  <https://orcid.org/0000-0003-3912-7503>

Department of Geophysics, Gümüşhane University, 29100, Gümüşhane, Türkiye

Department of Geophysics, Van Yüzüncü Yıl University, 65080, Van, Türkiye

INTRODUCTION

Spatial-temporal occurrences of earthquakes are not random and they generally occur without any precursors. These natural disasters are quite destructive and dangerous. Assuming that the crust of the earth is quite complex and earthquake behavior is chaotic, earthquake forecasting can be considered on a statistical basis. Thus, statistical modeling of earthquake behavior assumes great importance in forecasting

future potential earthquakes (Rundle *et al.* 2002). In general, it is possible to distinguish two types of earthquake forecasts. The first one is based on experimental measurements of precursory variations, while the other one deals with statistical patterns of earthquake distribution (Holliday *et al.* 2007). A lot of research is performed to forecast earthquakes and to define their spatial-temporal behavior in Turkey and different regions of the world (e.g., Varatsos, Alexopoulos 1984; Turcotte 1991; Keilis-Borok 1996; Sobolev, Tyupkin

1997; Huang *et al.* 2001; Tiampo *et al.* 2002; Polat *et al.* 2002; Keilis-Borok, Soloviev 2003; Holliday *et al.* 2005; Öncel, Wilson 2007; Öztürk 2011, 2020; Scholz 2015; Luginbuhl *et al.* 2018; Ulukavak *et al.* 2020; Nanjo 2020; Beroza *et al.* 2021) applying different physical models, scaling laws, parameters, observations, and approaches.

Comprehensive spatial-temporal analyses of seismicity show that earthquake occurrences display chaotic behavior, and hence, complicated statistical tools are necessary to evaluate the randomness and distributions of earthquakes. The frequency-magnitude relation (*b*-value) of the Gutenberg-Richter (G-R) scaling law (Gutenberg, Richter 1944) is one of the best-known and most frequently used tools in earthquake statistics. Literature survey indicates that *b*-value is related to the relative proportion of both small and great earthquakes. Also, it reflects the seismotectonic structure and the region-time-depth variations of stress (Utsu 1971). Therefore, by analyzing *b*-value, the fractal correlation between some variables such as the frequency of earthquakes, fault length, seismic energy, and seismic moment can be established. The G-R relationship is applied in numerous earthquake studies in different regions of the Earth (e.g., Smith 1981; Olsson 1999; Enescu, Ito 2002; Scholz 2015; Yaghmaei-Sabegh, Gholamreza 2021). These studies propose that the fractal behavior of earthquake occurrences may be related to seismogenic stress conditions throughout the earthquake activity and be also correlated with successive earthquake occurrences.

Besides the frequency-magnitude relation, abnormal spatial (regional)-temporal variations in earthquake occurrence rates are also considered to be precursors of seismic events. One of such indicators is the precursory seismic quiescence defined as a notable decline in the mean earthquake activity rate as against the background activity in a limited part of a seismotectonic region (Wiemer, Wyss 1994). A lot of research is available on the phenomenon of the precursory quiescence preceding the mainshock. According to these studies, several years before the mainshock, a significant decrease in seismicity is observed in focal regions (Wiemer, Wyss 1994; Console *et al.* 2000; Öztürk 2011, 2020; Puangjaktha, Pailoplee 2018; Derode *et al.* 2021; Öztürk, Alkan 2022a). Thus, as a technique for earthquake forecasting, the evaluation of seismic quiescence can provide advance information about the local tectonic evolution and the forthcoming seismic hazard (Bowman, King 2001).

The static changes in stress caused by a seismic event can change the current stress state and trigger a successive earthquake occurrence on a neighboring fault. Recent studies indicate that earthquakes cause stress distributions in the crust and this process can trigger earthquakes on nearby faults (e.g., Stein *et al.*

1997; Nalbant *et al.* 2002; Toda *et al.* 2005; Ozer, Polat 2017; Ahadov, Jin 2019; Alkan *et al.* 2021; Li, Chen 2021; Öztürk, Alkan 2022b). Coulomb stress variations were estimated following the Okada model (1985) by analyzing elastic dislocations on rectangular planes in a homogeneous and isotropic semi-space. Tectonic stress along the fault is assumed to change over time. Stress may increase throughout the loading cycle before large earthquake events and may quickly abate. Thus, earthquake-induced crustal deformation causes stress disturbance in and around the earthquake region. From the viewpoint of earthquake physics, the possible location of the next great earthquake depends on the condition of the stress loaded by previous earthquakes and the existing seismotectonic conditions (Nanjo 2020). Therefore, stress changes are significant for earthquake interactions and can be used for the preliminary earthquake forecasting.

The pattern informatics (PI) method is recommended as an alternative technique for forecasting earthquakes in addition to the G-R relation, precursory seismic quiescence, and stress analyses (Rundle *et al.* 2002; Tiampo *et al.* 2002). Reliability of the PI technique depends on the accurate evaluation of spatial-temporal earthquake distribution. This forecasting method can be applied for identifying the precursory seismic quiescence (Nanjo *et al.* 2006a). The results obtained applying this method are used in producing maps of seismogenic regions, where earthquakes are forecast to occur in the future (five to ten years ahead) (Holliday *et al.* 2006).

Relative Intensity (RI) is another alternative method used for forecasting earthquakes and may determine the possible regions of the next earthquake occurrences. The combined application of PI and RI techniques for earthquake forecasting yielded significant results, which allowed predicting potential seismic events in the study region more accurately (Holliday *et al.* 2005, 2006). The use of these two types of retrospective earthquake forecasting techniques in combination with the analyzed spatial-temporal patterns of the past events may allow predicting potential upcoming earthquake events.

Turkey is one of the best-investigated seismotectonic parts of the Earth. Therefore, there are a lot of comprehensive studies performed on earthquake behavior patterns in different earthquake source zones in Turkey. The East Anatolian region (EAR), which is one of the most active zones in Turkey, has a significant seismotectonic potential as regards the occurrence of great earthquakes in the medium and long term. Also, some destructive earthquakes occurred in Van and adjacent regions in the past and in recent years, e.g., April 29, 1903 Malazgirt ($M_s = 6.7$, surface wave magnitude), September 10, 1941 Erciş-Van ($M_s = 5.9$), February 26, 1960 Başkale-Van

($M_s = 5.8$), November 24, 1976 Muradiye-Van ($M_s = 7.5$), June 25, 1988 Van Lake ($M_s = 5.3$), November 15, 2000 Gevaş-Van ($M_s = 5.0$), October 23, 2011 Van ($M_s = 7.2$), June 24, 2012 Karagündüz-Van ($M_s = 5.0$) and December 6, 2021 Van Lake ($M_s = 5.0$) (Bogazici University, Kandilli Observatory and Research Institute, KOERI). Although there are many different studies conducted on seismicity in the Lake Van region, studies focusing on the imminent earthquake forecasting in this part of EAR are relatively few.

The principle aim of our study was to present different approaches to earthquake forecasting and hazard evaluation by performing spatial-temporal assessments of seismicity in the Lake Van region at the beginning of 2022. For that purpose, a comprehensive statistical evaluation of several seismotectonic parameters including the b -value of the G-R relation, Z -value of standard normal deviation (precursory seismic quiescence), and Coulomb stress changes was performed. Also, the applicability of the relative intensity and pattern informatics algorithms for forecasting strong earthquakes in this region was first assessed. It should be emphasized that the performed assessment of these parameters allowed obtaining significant findings for earthquake hazard forecasting and determination of the time and location of future earthquake occurrences in the Lake Van region.

TECTONIC STRUCTURES AND SEISMIC ACTIVITY IN VAN CITY AND ITS ADJACENT REGIONS

The tectonic structure of the EAR is the most complex in the Alpine-Himalayan orogenic system because it is affected by the active collision zone between the Eurasian and the Arabian plates. The N-S compressional tectonic regime of these main plates, which occurred in the past (~ 13 Ma), causes the crustal shortening and uplift in the EAR. This movement caused the westward escape and counter-clockwise rotation of the Anatolian plate along the dextral strike-slip North Anatolian Fault Zone (NAFZ) and the sinistral strike-slip East Anatolian Fault Zone (EAFZ). NAF and EAF zones intersect the Karlıova Triple Junction (KTJ). This recent compressional tectonic regime has caused many faults and fault segments with various earthquake focal mechanisms in the region (Fig. 1a). The Lake Van region is located southeast of KTJ (~ 125 km) and ~ 100 km north of the promontory thrust of the Bitlis-Zagros Thrust Zone (BZTZ) (McClusky *et al.* 2000; Bozkurt 2001; Keskinkin 2003; Şengör *et al.* 2003; Reilinger *et al.* 2006; Selçuk 2016; Alkan *et al.* 2020; Gülyüz *et al.* 2020; Kayın, İşseven 2023). At present, the Lake Van zone includes three deep sub-basins (Northern Basin,

Tatvan Basin, and Deveboynu Basin) and basement ridges (e.g., Northern, Ahlat). This region is characterized by oblique-slip boundary faults and a N-S shortened domal morphological structure (Çukur *et al.* 2017; Toker 2021).

Several active faults and fault zones around the Lake Van region were defined by Emre *et al.* (2013; 2018) as shown in Fig. 1b. The main tectonic structures in and around the study region include the faults and fault zones called Erciş, Çaldıran, Süphan, Nemrut, Nazik Gölü, Malazgirt, Yeniköşk and Saray, and Van. The Erciş, Çaldıran, Nazik Gölü, and Saray fault zones are controlled by the right-lateral strike-slip mechanism, while the mechanism underlying Süphan and Malazgirt faults is mainly left-lateral strike-slip. However, the Yeniköşk fault and the Van fault zone are controlled by reverse fault mechanisms typically trending E-W, whereas the Nemrut fault and the extension fissures of the Tendürek fault are characterized as normal fault systems. The Lake Van region is seismically very complex. It that has undergone numerous strong shallow earthquakes in the instrumental period. The most recent Van earthquake (October 23, 2011) caused great destruction in the region. This great earthquake generated a lot of aftershocks ($\sim 9,000$) and some of them had a strong magnitude reaching 5.6 on the Richter scale (Irmak *et al.* 2012; Utkucu *et al.* 2013; Selçuk 2016).

EARTHQUAKE DATABASE AND SHORT DESCRIPTIONS OF THE METHODS

This study presents part of the earthquake catalogue compiled by Öztürk (2009). It spans the time interval between 1970 and 2006 (for details see Bayrak *et al.*, 2009). This homogeneous database contains information on the duration magnitude (M_d) of 392 earthquake occurrences in the period from 1970 to 2006. In addition, in this study, we analyzed the data taken from KOERI (Bogazici University, Kandilli Observatory and Research Institute) on 13,786 earthquakes that occurred from 2006 to 2022. When selecting data for statistical analysis, preference was given to shallow earthquakes (depth < 70 km) because the seismogenic depth in the EAR study region is claimed to have changed from 40 to 45 km (Alkan *et al.* 2020). Hence, the total catalogue of the earthquakes discussed in this article lists 14,178 events with the magnitude in the range of $1.0 \leq M_d \leq 6.6$, which occurred in the period of approximately 51.09 years, i.e. between November 28, 1970, and December 31, 2021. The epicenter locations of these earthquakes are plotted in Fig. 2 using different symbols for different magnitude sizes.

The Coulomb stress variation was investigated us-

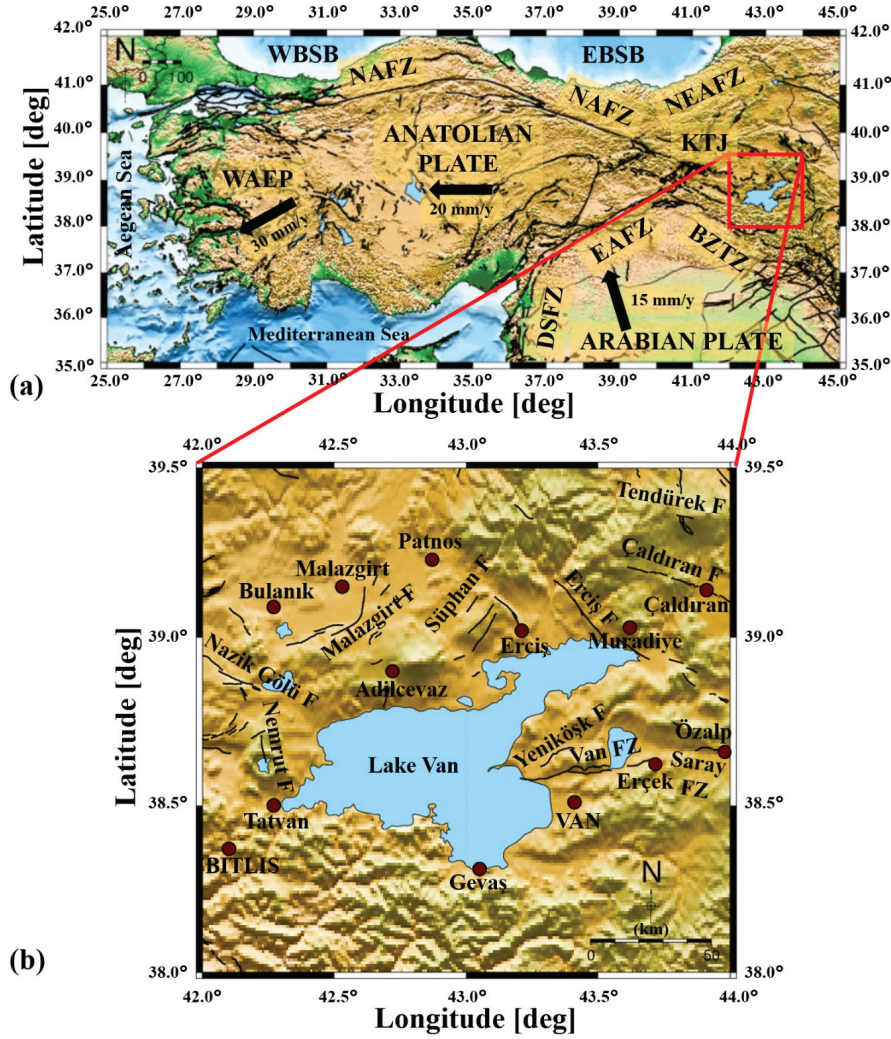


Fig. 1 (a) Tectonic structure in and around Turkey demonstrates the main neotectonics and provinces (modified from Bozkurt 2001; Emre *et al.* 2013, 2018). Large arrows indicate the general direction of the plate movement. The study region is presented in a red rectangular frame. Abbreviations: EBSB: the Eastern Black Sea Basin, WBSB: the Western Black Sea Basin, WAEP: the Western Anatolian Extensional Province, EAFZ: the Eastern Anatolian Fault Zone, NAFZ: the Northern Anatolian Fault Zone, NEAFZ: the Northeast Anatolian Fault Zone, BZTZ: the Bitlis-Zagros Thrust Zone, DSFZ: the Dead Sea Fault Zone, KTJ: the Karhova Triple Junction. (b) Active tectonic faults in Lake Van and its adjacent region (taken from Emre *et al.* 2018). Claret red circles mark city locations

ing the information on 66 earthquakes (moment magnitude, $M_w \geq 4.5$), which occurred in the Lake Van region between 2011 and 2021. The catalogue information on earthquakes (dip, strike, rake, etc.) presented in Table 1 was obtained from the AFAD (Disaster and Emergency Management Authority). Also, Fig. 3 shows the focal mechanism solutions and epicenter locations of all the events, which demonstrated strike-slip faults in general. Thus, the stress variations are analyzed based on the strike-slip fault mechanism.

Magnitude-frequency relation of the Gutenberg-Richter scaling law (b -value)

The empirical scaling law for earthquake occurrences was proposed by Gutenberg and Richter (1944). The basic formula for the frequency-magni-

tude relationship in earthquake statistics can be expressed as follows:

$$\log_{10} N(M) = a - bM \quad (1)$$

where $N(M)$ is the cumulative number of earthquake events with magnitudes equal to or greater than M during a certain time interval. The a - and b -values are positive constants; the b -value can be obtained from the slope of the frequency-magnitude distribution. However, the a -value is related to the seismicity rate. Changes in a -value for different regions are related to the period covered by the catalogue, size of the study region, and the number of earthquake events recorded. The b -value for different seismotectonic parts of the world (Utsu 1971) varies from 0.3 to 2.0, and the given average b -value fluctuates around 1.0 (Frohlich, Davis 1993). The b -value is stated to be

related to the relative distributions of small and great earthquakes. However, different factors such as tectonic features, anisotropic structure, and stress heterogeneities can cause b -value variations. There exists a negative relation between the b -value and stress distribution. Also, geological complexity, crack density, thermal gradient, material properties, fault length, seismic wave velocity changes, seismic attenuation, strain circumstances, and slip distribution are associated with variations in b -value (Mogi 1962; Schorlemmer *et al.* 2005; Scholz 2015). Seismic activity is characterized by relatively high b -values in magmatic zones. Therefore, small effective stress variations can be related to high pore pressures and geothermal gradients (Abdelfattah *et al.* 2020). Thus, b -value is a crucial parameter indicating the potential for earthquake occurrences in the region.

The estimation of b -value, mapping of the precursory seismic quiescence, and estimation of the completeness magnitude (M_{comp}) are very important for obtaining reliable and high-quality statistical results. The latter type of estimation must be done before other analyses. M_{comp} can be defined as the minimum magnitude above which all earthquakes within a certain region are reliably recorded. It can be estimated from the frequency-magnitude distribution of events (Wiemer, Wyss 2000).

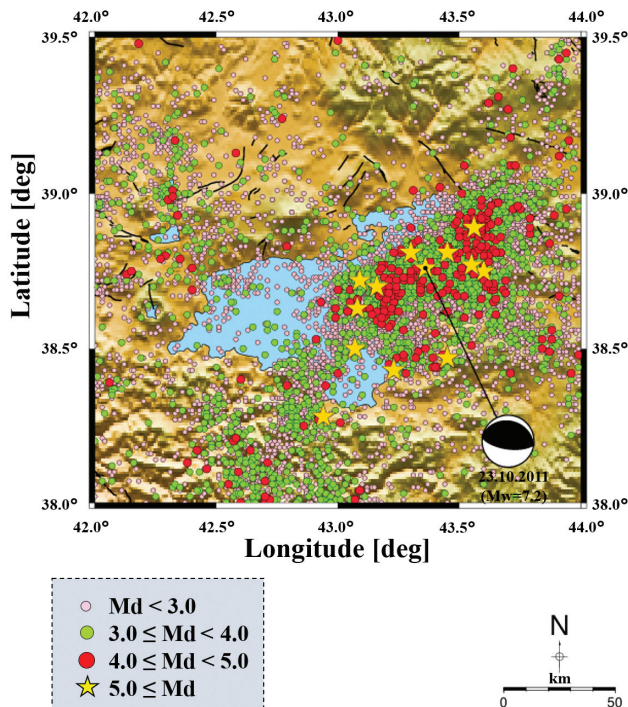


Fig. 2 Epicenter distributions of 14,178 shallow earthquake occurrences with $M_d \geq 1.0$ in the Lake Van region in the period 1970–2022 that are included in the original catalogue. The magnitude of earthquakes is represented using different symbols (Catalogue information on earthquakes is taken from KOERI). The fault plane solution demonstrates the focal mechanism of the 2011 Van earthquake ($M_w = 7.2$)

90% of the earthquake events listed in the catalogue exceed the magnitude of completeness. M_{comp} variations over time can affect statistical outputs, and hence, the maximum number of events must be used to achieve correct estimations. As M_{comp} value is used in several analyses, M_{comp} changes over time are examined first.

Declustering Process and Standard Normal Deviate (Z-value, Precursory Seismic Quiescence)

One of the most important stages in compiling quantitative earthquake statistics for the assessment of seismicity rate changes and earthquake hazard analyses is the procedure of separating secondary earthquake events (earthquake swarms, foreshocks, or aftershocks) from the primary ones and excluding them from earthquake catalogues (Mizrahi *et al.* 2021). During declustering, all the main events are removed from each cluster and all primary earthquakes are recorded as a single event. Thus, to ensure the uniformity of the data to be used in earthquake forecasting models, the catalogue of earthquake events must undergo the declustering procedure. In our study, the catalogue was declustered following Reasenber (1985) and applying the ZMAP (Wiemer 2001) packaged software.

According to the seismic quiescence hypothesis, which was put forward by Wyss and Habermann in 1988, an earthquake is preceded by a significant decrease in earthquake activity, otherwise known as precursory quiescence, in a limited part of the seismogenic zone (Wiemer, Wyss 1994). There exist

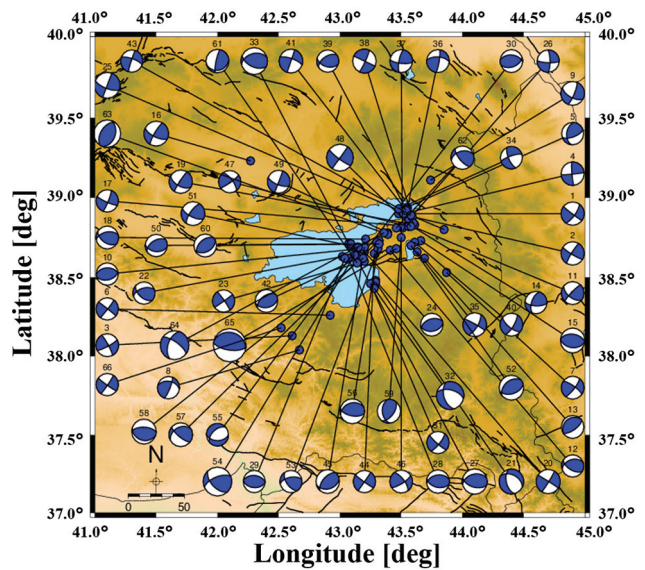


Fig. 3 The fault plane solutions were calculated based on the events that occurred in the Lake Van region (See Table 1 for details). Focal mechanism parameters were taken from the AFAD website (URL-1, DDA Catalog (<https://deprem.afad.gov.tr/ddakatalogu?lang=en>))

Table 1 Focal mechanism results for the earthquake occurrences in the study region (38.0°N–39.5°N latitude and 42.0°E–44.0°E longitude) between 2011 and 2022. Focal mechanism solutions were taken from the AFAD website (URL-1, DDA Catalog, afad.gov.tr)

No	Date (UTC)	Latitude (°N)	Longitude (°E)	Magnitude (Mw)	Depth (km)	Strike (°)	Dip (°)	Rake (°)
1	05/12/2021 21:46:47	38.906	43.485	4.7	7.62	127	87	-163
2	14/12/2020 21:58:45	38.901	43.487	4.7	9.2	212	82	8
3	07/08/2020 19:20:13	38.131	42.613	4.6	6.99	331	83	171
4	03/04/2020 05:44:24	38.909	43.529	4.7	12.99	175	85	3
5	14/06/2018 15:42:21	38.941	43.555	4.5	13.66	187	45	36
6	01/05/2017 16:30:40	38.265	42.928	4.5	12.44	308	88	177
7	23/11/2016 12:14:36	38.539	43.870	4.6	9.97	305	76	167
8	23/01/2016 07:53:44	38.049	42.670	4.5	15.21	279	42	163
9	29/10/2015 09:46:39	39.119	43.743	4.8	4.9	119	61	-167
10	23/06/2015 22:35:20	38.681	43.179	4.5	30.45	268	44	97
11	18/02/2014 21:51:35	38.836	43.563	4.6	11.67	224	81	34
12	21/09/2013 02:15:44	38.673	43.418	4.5	17.03	252	42	50
13	12/06/2013 19:02:51	38.624	43.690	4.6	15.91	232	23	87
14	24/11/2012 16:04:28	38.833	43.572	4.5	17.53	93	66	145
15	24/06/2012 20:07:21	38.733	43.667	5.0	23.62	96	42	89
16	26/03/2012 10:35:33	39.234	42.276	5.0	16.96	116	67	168
17	24/02/2012 13:07:10	38.827	43.565	4.5	22.09	22	82	-10
18	17/02/2012 09:32:57	38.743	43.216	4.6	7.02	258	50	56
19	06/12/2011 02:55:59	38.833	43.616	4.7	15.36	119	58	172
20	04/12/2011 22:15:03	38.481	43.299	4.9	12.22	32	86	2
21	30/11/2011 00:47:21	38.470	43.290	5.0	19.79	166	56	-58
22	24/11/2011 00:48:07	38.633	43.028	4.5	15.9	253	53	47
23	22/11/2011 03:30:35	38.609	43.200	4.5	22.95	55	88	6
24	21/11/2011 20:55:56	38.669	43.205	4.6	22.74	82	42	97
25	18/11/2011 17:39:39	38.802	43.852	5.2	8.0	201	90	20
26	17/11/2011 12:38:31	38.867	43.569	4.5	17.1	92	78	-166
27	14/11/2011 22:08:14	38.703	43.083	5.1	23.32	256	41	66
28	14/11/2011 16:47:16	38.624	43.075	4.7	18.98	103	49	105
29	14/11/2011 16:31:31	38.621	43.040	4.5	19.21	95	45	90
30	12/11/2011 18:20:01	38.632	43.173	4.6	19.15	71	47	73
31	09/11/2011 20:45:38	38.464	43.253	4.5	17.74	39	77	-9
32	09/11/2011 19:23:34	38.438	43.282	5.6	21.47	163	52	-44

No	Date (UTC)	Latitude (°N)	Longitude (°E)	Magnitude (Mw)	Depth (km)	Strike (°)	Dip (°)	Rake (°)
33	08/11/2011 22:05:50	38.719	43.077	5.4	8.36	255	43	59
34	07/11/2011 22:14:12	38.935	43.483	4.5	14.63	156	69	-14
35	07/11/2011 15:54:48	38.663	43.632	4.8	4.43	31	69	5
36	06/11/2011 02:43:12	38.939	43.554	4.6	11.66	9	81	30
37	05/11/2011 19:19:15	38.814	43.513	4.6	22.03	191	74	17
38	02/11/2011 04:34:21	38.884	43.590	4.8	18.03	25	84	0
39	01/11/2011 21:10:44	38.846	43.609	4.5	5.06	237	54	56
40	30/10/2011 01:55:04	38.729	43.612	4.6	22.36	31	73	-23
41	29/10/2011 22:24:22	38.924	43.543	4.8	16.67	199	90	-18
42	29/10/2011 18:45:49	38.622	43.152	4.6	13.97	80	42	110
43	28/10/2011 16:34:10	38.897	43.583	4.5	12.44	198	86	-18
44	26/10/2011 16:19:44	38.659	43.285	4.5	1.45	35	89	-3
45	26/10/2011 03:16:18	38.692	43.200	4.8	20.62	222	57	70
46	26/10/2011 02:59:05	38.828	43.506	4.6	14.81	58	75	22
47	25/10/2011 15:27:13	38.826	43.566	4.5	16.01	55	83	21
48	25/10/2011 14:55:06	38.823	43.585	5.4	17.44	36	89	-9
49	24/10/2011 23:55:15	38.787	43.390	4.6	26.37	21	89	-22
50	24/10/2011 22:13:30	38.713	43.097	4.5	19.24	239	52	65
51	24/10/2011 15:28:06	38.693	43.147	4.8	18.71	215	70	25
52	24/10/2011 08:49:19	38.706	43.582	5.0	17.27	231	43	73
53	24/10/2011 04:18:45	38.680	43.310	4.5	12.58	145	57	141
54	23/10/2011 20:45:34	38.644	43.127	5.8	6.79	137	55	147
55	23/10/2011 19:43:24	38.697	43.150	4.5	7.55	228	52	-119
56	23/10/2011 19:06:05	38.735	43.328	5.0	22.09	252	34	65
57	23/10/2011 18:53:47	38.724	43.302	4.8	6.08	129	74	124
58	23/10/2011 18:10:44	38.629	43.192	5.0	19.81	106	30	102
59	23/10/2011 16:05:10	38.751	43.508	4.8	20.85	175	43	57
60	23/10/2011 15:57:59	38.717	43.326	4.6	21.78	63	43	100
61	23/10/2011 15:24:29	38.590	43.149	4.7	21.55	77	22	153
62	23/10/2011 13:17:03	38.811	43.467	4.7	15.41	140	68	128
63	3/10/2011 11:32:40	38.777	43.394	5.5	22.61	213	51	99
64	23/10/2011 10:56:48	38.782	43.363	5.8	19.92	305	71	-140
65	23/10/2011 10:41:20	38.689	43.465	6.7	19.02	98	66	88
66	30/04/2011 15:26:03	38.183	42.525	4.5	5.0	125	86	-176

many different methods for identifying and characterizing seismicity rate changes. Most of them are based on the spatial-temporal modeling of the seismic quiescence before the mainshocks. The algorithm provided by the *ZMAP* computer program was devised by Wiemer and Wyss (1994). The *ZMAP* technique is used to monitor the areas exhibiting the period of quiescence in earthquake activity. *Z*-test generates the Long-Term Average, $LTA(t)$ function for the statistical evaluation of the confidence level in standard deviation units:

$$Z(t) = \frac{R_1 - R_2}{\left[\left(\sigma^2_1 / n_1 \right) + \left(\sigma^2_2 / n_2 \right) \right]^{1/2}} \quad (2)$$

where R_1 is the mean activity rate in the overall foreground period, R_2 is the mean activity rate in the background period, σ is the standard deviation and n is the number of the sample within and outside the window. *Z*-value is estimated as a function of time. Thus, *Z*-value lets the foreground window slide along the time interval of the catalogue and is called $LTA(t)$.

Relative Intensity (RI), Pattern Informatics (PI), and Forecast Map Creation

Another way of earthquake forecasting is based on the analyses of the occurrence rate of small past earthquakes and regions exhibiting high seismic activity and/or quiescence. Large earthquake events are followed by a sequence of smaller events, i.e. aftershocks, caused by release of residual stress. They steadily decrease in magnitude and frequency and are instrumentally detectable in the area until a successive earthquake hits (Holliday *et al.* 2007). In relation to this process, the combined application of PI and RI techniques for earthquake forecasting has recently yielded significant results. Although the application of these techniques cannot guarantee the prediction of earthquakes, their combined use can forecast the seismogenic areas (hot spots) where earthquakes can be expected to occur in the period of the next 5–10 years.

RI and PI algorithms are used in numerous studies dealing with earthquakes and their prediction (Nanjo *et al.* 2006a, b; Holliday *et al.* 2005, 2006, 2007). The essence of the relative intensity (RI) method used in this study can be described as follows (see Nanjo *et al.* 2006b for details):

- a. The study area is divided into a grid of boxes with a linear dimension Δx .
- b. The number of events with a magnitude M_d equal to or larger than M_{comp} value in box j is calculated for the period between t_s and t_E . t_s and t_E are the starting and ending times of the earthquake events listed in the catalogue, respectively. This number is averaged to deter-

mine the number of events per day, denoted as $n_j(t_s, t_E)$.

- c. The relative value of $n_j(t_s, t_E)$ is defined as the RI score. It is described as $n_j(t_s, t_E)/n_{MAX}$. The largest value of $n_j(t_s, t_E)$ is n_{MAX} and thus, RI value changes between 0 and 1.
- d. When considering the threshold value of w from zero to one ($0 \leq w \leq 1$), the next large events are expected to occur only in boxes of RI values higher than w -value. The boxes of RI values lower than the threshold w -value are accepted as the regions where the next large events are not forecast to occur.
- e. According to the RI model, great events are most likely to occur in the regions of more intense earthquake activity.

The essence of the PI method and algorithm used in this study can be conveyed as follows: (see Nanjo *et al.* 2006b for details):

- a. As in the case of RI method, the study area is divided into a grid of boxes with a linear dimension Δx .
- b. All the events with the magnitude M_d equal to or larger than M_{comp} value ($M_d \geq M_{comp}$), recorded in the study area from time t_0 , are included.
- c. The analysis focuses on three time periods:
 - 1) The reference time between t_b and t_1 .
 - 2) The period between t_b and t_2 ($t_2 > t_1$). The change period, during which seismicity variations are observed, is between t_1 and t_2 . The time t_b is between t_0 and t_1 . The aim is to determine abnormal earthquake activity in the change period from t_1 to t_2 relative to the reference period from t_b to t_1 .
 - 3) The forecast period from t_2 to t_3 is the period for which the forecast is valid.
- d. The earthquake intensity in the box for the period is the average number of events with $M_d \geq M_{comp}$ that occurred throughout this period. The earthquake intensity in the box j during the reference period from t_b to t_1 denoted as $n_j(t_b, t_1)$, is the average number of events that occurred between t_b and t_1 . The earthquake intensity in the box j during the period from t_b to t_2 denoted as $n_j(t_b, t_2)$, is the average number of events that occurred between t_b to t_2 .
- e. To allow the comparison between seismic intensities during two different time periods, they are required to have the same statistical features. Hence, the earthquake intensities are normalized by subtracting the average seismicity from all the boxes and dividing the average seismicity by the standard deviation of the seismicity in all the boxes. These normalized

- intensities are denoted as $n_j(t_b, t_1)$ and $n_j(t_b, t_2)$.
- f. The degree of abnormal earthquake activity in the box j is given as the difference between two normalized earthquake intensities, $\Delta n_j(t_b, t_1, t_2) = n_j(t_b, t_2) - n_j(t_b, t_1)$.
 - g. To diminish the relative significance of random fluctuations in seismicity, the average change $\Delta n_j(t_b, t_1, t_2)$ is calculated for all possible initial times t_b between t_0 and t_1 . The result is given as $\Delta \underline{n}_j(t_0, t_1, t_2)$.
 - h. The possibility of the next event in the box j is given as $P_j(t_0, t_1, t_2)$. It is defined as the square of the intensity variation, $P_j(t_0, t_1, t_2) = \{\Delta \underline{n}_j(t_0, t_1, t_2)\}^2$.
 - i. To denote abnormal areas, it is necessary to calculate the variation in the possibility $P_j(t_0, t_1, t_2)$ relative to the background activity. This means that the average probability is subtracted from all boxes $\langle P_j(t_0, t_1, t_2) \rangle$. This variation in the possibility is expressed as $P'_j(t_0, t_1, t_2) = P_j(t_0, t_1, t_2) - \langle P_j(t_0, t_1, t_2) \rangle$.
 - j. The relative possibility value is defined as PI score. This is formulized with $P'_j(t_0, t_1, t_2) / P_{MAX} \cdot P_{MAX}$ is the greatest value of $P'_j(t_0, t_1, t_2)$ since it is related to the seismic quiescence/activation relative to the background seismicity. These values are replaced by zero if boxes have PI values smaller than zero. Thus, PI value changes between 0 and 1.
 - k. If a threshold w -value is accepted to vary between 0 and 1, the next large events in boxes of PI values are expected to be greater than this w -value. The boxes of PI values lower than the threshold w -value are the regions where the next large events are not forecast to occur.
 - l. According to the PI model, great earthquakes are expected to occur in areas with higher earthquake quiescence or activity.

The results obtained applying the PI method indicate the areas where earthquakes are most likely to occur in the future. PI and RI maps are combined to create a forecast map. This map is then renormalized to obtain the earthquake probability for the future 5 to 10-year period (see Holliday *et al.* 2007 for details):

- a. As a first step, a relative intensity map is created for all the areas. Then, relative values higher than 10^{-1} are adjusted to 10^{-1} , and nonzero values smaller than 10^{-4} are adjusted to 10^{-4} . In the end, every box with zero historic earthquake activity is set to 10^{-5} .
- b. The PI values are calculated over the top 10% of the most active parts of the study region. The times t_0 , t_1 , and t_2 are defined for the calculations. Since future events are expected to occur in hotspots, they are stated with probability values.

- c. Finally, a composite forecast map is created by superimposing the Pattern Informatics map and its Moore neighborhood (the pixel + its eight adjacent neighbors) onto the Relative Intensity map. Entire hotspot pixels have a possibility of 1 and, all other pixels have possibilities that vary from 10^{-5} to 10^{-1} .

Coulomb stress changes

Coulomb stress analysis is a well-established approach to studying stress conditions under which failures occur in source faults. Dependence of the Coulomb failure stress ($\Delta\sigma_{cfs}$) change on the receiver fault can be expressed as follows:

$$\Delta\sigma_{cfs} = \Delta\tau_s + \mu'\Delta\sigma_n \quad (3)$$

Here, $\Delta\tau_s$ represents the shear stress variation associated with the positive direction of the receiver fault slip, $\Delta\sigma_n$ is the normal stress change along the fault plane and μ' is the effective coefficient of friction on the fault (Toda *et al.* 2011). μ' includes the effects of pore-pressure changes and varies between 0 and 1. For the calculation of stress changes, μ' -value was taken as 0.4 as stated in King *et al.* (1994). We assume that the dimensionless Poisson's ratio (ν) is 0.25 and Young modulus (E) is chosen as 8×10^5 bars. The Coulomb stress changes from -0.1 to 0.1 (bar) are considered to record the forthcoming earthquake hazards (Yadav *et al.* 2012). The positive Coulomb stress variation shows the loading of stress, pushing the fault towards brittle failure, whilst negative changes in the Coulomb stress distribution correspond to the unloading stress, inhibiting the rupture of the earthquake (Stein *et al.* 1994; Liao *et al.* 2022).

RESULTS

The detailed analysis and forecasting of the earthquake hazard in the Lake Van region, an important seismic hazard region in Turkey, was performed using multiple parameters: (i) the b -value of G-R relation, (ii) the precursory quiescence Z -value, (iii) Coulomb stress variations (iv) RI, PI, and their combination. For this purpose, the spatial-temporal behavior of earthquake occurrences was mapped for the beginning of 2022.

For the determination of the minimum magnitude to be used in spatial-temporal seismicity analyses, the estimation of M_{comp} , which shows variations of completeness over time, must be done as a first step. However, the principal aim of this analysis was to ensure the statistical reliability of calculations by using the maximum number of events. Woessner, Wiemer (2005) stated that M_{comp} variations over time can be calculated by using a moving time window technique.

In this study, temporal M_{comp} variations with their standard deviations were obtained for every 250 samples per window. The original catalogue containing 14,718 $M_d \geq 1.0$ earthquake events was used in this study. The variation of M_{comp} over time was plotted in Fig. 4. Until 2011, the range of M_{comp} variation was 2.8–3.3. At the beginning of 2012, it decreased to about 2.5, and since 2012, it has been fluctuating between 2.0 and 2.5. Thus, temporal M_{comp} variations are not stable and there was a clear fluctuation between 2.0 and 3.3 recorded in the period 1970–2022. It can be concluded that $M_{comp} = 2.5$ is consistent with the findings of our previous studies (Öztürk 2017, 2018) and is suitable for the analyses. Since this study includes b -value, Z -value, RI, and PI statistics, M_{comp} analysis is conducted as a first step and 2.5 is used as the average M_{comp} value in all statistical estimations.

As stated above, the original earthquake catalogue lists 14,178 $M_d \geq 1.0$ shallow earthquake events recorded over the period 1970–2022. As a result of the performed catalogue declustering, 5449 earthquakes (nearly 38.43%) were removed from it. When examining the original database, M_{comp} was set equal to 2.5. The $M_d < 2.6$ earthquake events, which were 4934 in number, were removed from the database. After declustering, $\sim 73.24\%$ of the original catalogue was eliminated. Thus, the number of earthquakes decreased to 3794. This uniform and independent database was used for seismic quiescence analysis.

Fig. 5 shows the cumulative number of earthquake occurrences over the time period indicated in the catalogue. This catalogue lists 14,178 $M_d \geq 1.0$ earthquakes. In addition to this original database, the declustered catalogue including 8729 $M_d \geq 1.0$ earthquakes and the declustered catalogue listing 3794 $M_d \geq 2.5$ earthquakes were represented in Fig. 5. There were no significant fluctuations in seismicity recorded during the period 1970–2001, and very few seis-

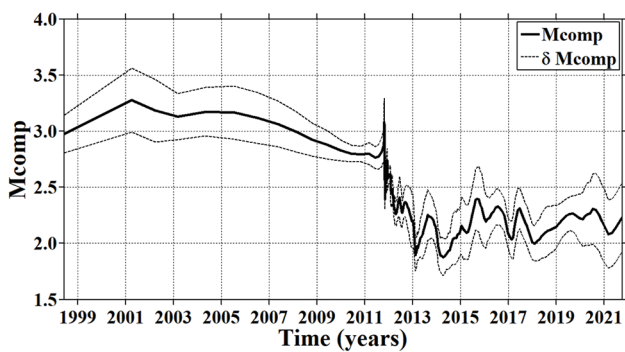


Fig. 4 Temporal variation of magnitude completeness, M_{comp} , from 1970 to 2022. The standard deviation, δM_{comp} , was also plotted. M_{comp} value was determined using the moving window technique, each window consisting of 250 events

mic events were observed in the period 2001–2012. However, a significant increase in the number of earthquakes was recorded after the 2011 Van earthquake. As seen in Fig. 5, the cumulative number of declustered earthquake events with $M_d \geq 2.5$ have a smoother slope than those listed in the original database. Literature surveys show that M_{comp} analysis and catalogue declustering are necessary both for the removal of dependent earthquakes such as aftershocks, foreshocks, or swarms from catalogues and for the statistical assessment of earthquake behavior (Katsumata, Kasahara 1999; Joseph *et al.* 2011). The catalogue is ready to be used for statistical spatial-temporal earthquake analyses after it has been declustered and $M_d < 2.6$ earthquakes have been removed from it.

Fig. 6 shows b -value and its regional variations. It is computed based on the original catalogue, including 14,178 earthquake events, and the maximum likelihood estimation with the M_{comp} ($M_{comp} = 2.5$) value set equal to 2.5. As seen in Fig. 6a, b -value is equal to 1.08 ± 0.07 with its standard deviation. On a global scale, b -value fluctuates between 0.3 and 2.0, and tectonic events are suggested when b -value is within the range of 0.5–1.5, although the average b -value is close to 1.0. Therefore, the b -value of earthquake distribution in the Lake Van region is well represented by the G-R scaling law with the b -value close to 1.0. The regional variation of b -value is presented in Fig. 6b, which was plotted using a moving window technique in $ZMAP$ with a sample of 850 earthquakes per window. This map was prepared considering a spatial grid of $0.02 \times 0.02^\circ$ for longitude and latitude. The analysis of the declustered catalogue of $M_d \geq 2.5$ earthquakes revealed that the regional b -value varies within the range of 0.85–1.22. According to Frohlich and Davis (1993), the b -value suggesting earthquake occurrences is well represented by the G-R relation

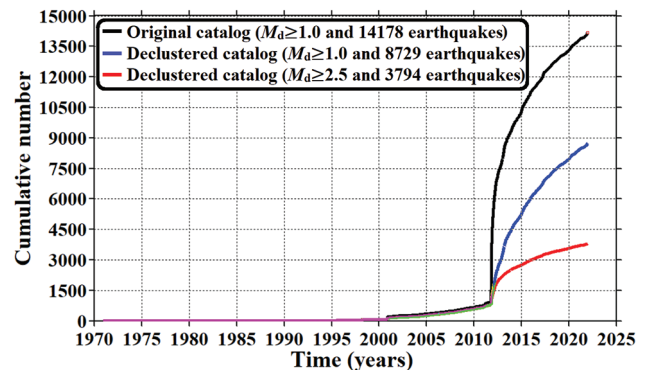


Fig. 5 Time variations of the cumulative number of earthquakes between 1970 and 2022 for the original database of earthquakes with $M_d \geq 1.0$ (black line), for the declustered database of earthquakes with $M_d \geq 1.0$ (blue line), and for the declustered database of earthquakes with $M_d \geq 2.5$ (red line)

with an average value of $b = 1.0$. According to this explanation, the areas exhibiting higher b -values (> 1.0) are located in western, northwestern, southern, and southwestern parts of the Lake Van region, including Patnos, Malazgirt, Bulanık, Tatvan, Adilcevaz, Gevaş, Erciş and covering Süphan, Malazgirt, Nazik Gölü, Nemrut faults. On the contrary, the regions with lower b -values (< 1.0) are generally located in the northern, northeastern, eastern, and southeastern parts of the Lake Van region including Çaldıran, Muradiye, Özalp, Erçek, and Van city center that are located along the faults Tendürek, Çaldıran, Erciş, and Yeniköşk, Van, and Saray (Fig. 6b). The regions with higher b -values generally experience a great number of small-magnitude earthquakes, whereas lower b -values are determined in the regions where large-magnitude events generally occur (Fig. 2). Consequently, the b -value, as estimated from the G-R relation, shows a clear relationship with the seismic and tectonic structure.

As stated above, the identification of precursory quiescence in earthquake activity showing the rate of seismicity in a region may provide credible evidence for earthquake forecasting. For this purpose, as in

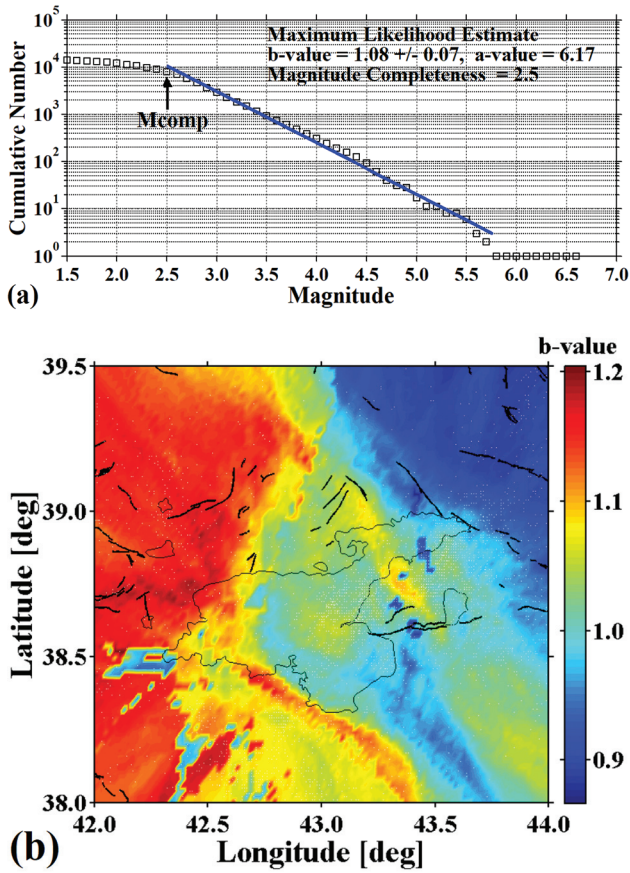


Fig. 6 (a) The Gutenberg-Richter scaling law and b -value of frequency-magnitude relation. b -value, its standard deviation, a -value, and M_{comp} were also presented. **(b)** Spatial variations in b -value for the Lake Van region. White dots indicate the declustered events with $M_d \geq 2.5$

the case of the b -value calculation, the study region is divided into rectangular grids of $0.02 \times 0.02^\circ$ in latitude and longitude. The time window length (T_w) selected for Z -value mapping is 5.5 years, because this time length enhances the visibility of quiescent regions. The declustered data on 3794 earthquakes with $M_d \geq 2.5$ were used to map the regional distribution of Z -value. Figs 7a–7i show spatial variations of the standard normal deviate (Z -value) in the period 2012–2022. As shown in Figs. 7a–7i, spatial variations of Z -value were mapped every six months from 2012 to 2022 by adding time intervals $T_w = 5.5$ years to the chosen time. These years were indicated as “cut at” time on Figs 7a–7i. The current Z -value map produced at the beginning of 2022 is presented in Fig. 7j. These figures show spatial-temporal variations of Z -values with the beginning of quiescence. Figs 7a–7i show that in the period 2012–2018, there was no notable quiescence recorded in the regions of seismic activity. However, these maps indicate some regions of clear quiescence that became apparent after 2018, and especially in the period between 2020 and 2022. As seen in Fig. 7j, at the beginning of 2022, there existed six quiescence regions. At the beginning of 2022, the regions of seismic quiescence were concentrated at (a) 39.10°N – 42.36°E (region A, between Malazgirt and Bulanık provinces covering the Malazgirt fault), (b) 38.97°N – 43.08°E (region B, between Patnos and Erciş provinces encompassing the Süphan fault), (c) 38.94°N – 43.84°E (region C, between Muradiye, Çaldıran and Özalp provinces covering the Çaldıran and Saray fault zones), (d) 38.48°N – 43.52°E (region D, between Van and Erçek provinces covering the Yeniköşk and Van fault zones), (e) 38.54°N – 42.91°E (region E, the southern part of Lake Van and the northwestern part of Gevaş province) and (f) 38.68°N – 42.36°E (region F, north of Tatvan province covering the Nemrut fault). Thus, these regions of the seismic quiescence anomaly may be significant, and the results obtained from the comprehensive Z -test can enhance the reliability of precursors in earthquake forecasting in the region.

In the framework of this study, a composite forecast map for the Lake Van region and its adjacent regions was created by combining the RI map (Fig. 8a) and PI map (Fig. 8b). As in the cases of b -value and Z -value maps, rectangular grid spaces of $0.02 \times 0.02^\circ$ in latitude and longitude ($\Delta x = 0.02^\circ$) representing the study region were investigated. M_{comp} value was taken equal to 2.5 as in the cases of b -value and Z -value maps. Then, the great earthquake events that were recorded during the forecast period (defined in the “Methods” section) were described by the total number of $M_d \geq 5.0$ events expected over the next ten years. Finally, the times (t_s , t_E , t_0 , t_1 , t_2 , t_3) and time intervals (forecast and change periods) were defined.

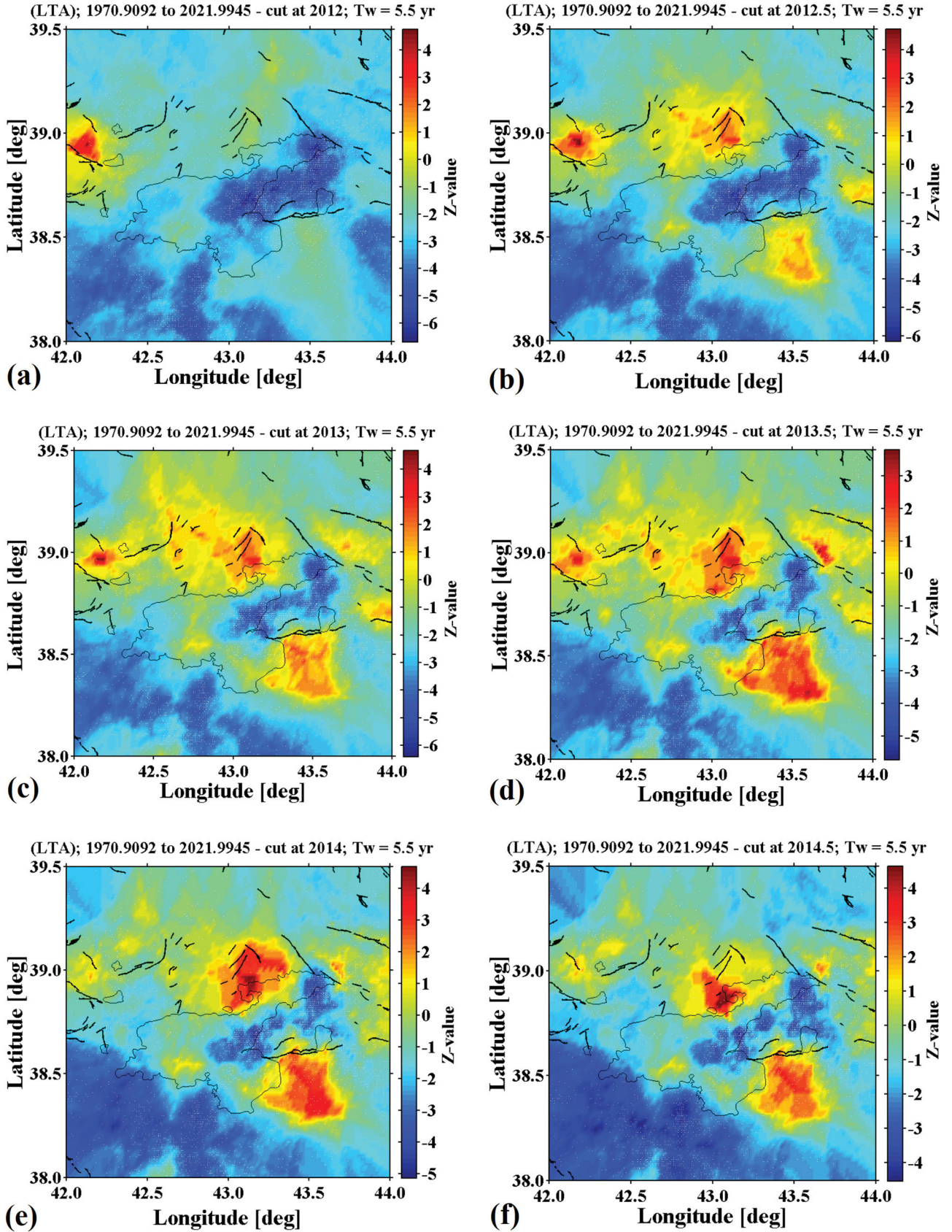


Fig. 7 Regional variations in Z-value for every six months between 2012 and 2022: (a) between 2012 and 2017.5, (b) between 2012.5 and 2018, (c) between 2013 and 2018.5, (d) between 2013.5 and 2019, (e) between 2014 and 2019.5, (f) between 2014.5 and 2020, (g) between 2015 and 2020.5, (h) between 2015.5 and 2021, (i) between 2016 and 2021.5, (j) between 2016.5 and 2022. Figure 7j represents the quiescence regions detected at the beginning of 2022. Declustered events with $M_d \geq 2.5$ were used and represented with white dots. The set time window is $T_w = 5.5$ years

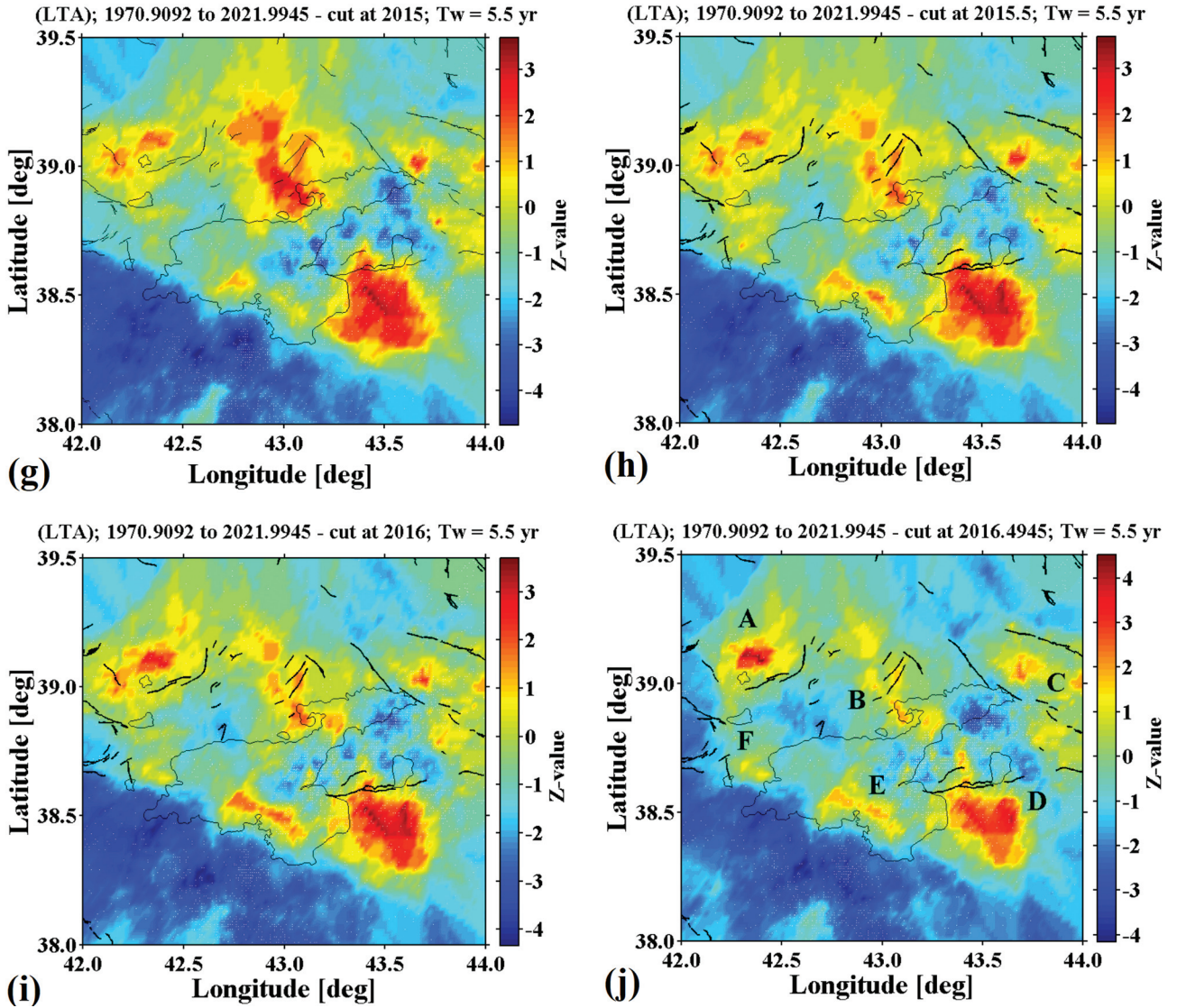


Fig. 7 Regional variations in Z-value for every six months between 2012 and 2022: (a) between 2012 and 2017.5, (b) between 2012.5 and 2018, (c) between 2013 and 2018.5, (d) between 2013.5 and 2019, (e) between 2014 and 2019.5, (f) between 2014.5 and 2020, (g) between 2015 and 2020.5, (h) between 2015.5 and 2021, (i) between 2016 and 2021.5, (j) between 2016.5 and 2022. Figure 7j represents the quiescence regions detected at the beginning of 2022. Declustered events with $M_d \geq 2.5$ were used and represented with white dots. The set time window is $T_w = 5.5$ years

The period between January 1, 2022 and January 1, 2032 was selected as a forecast interval. The analyzed interval of seismic activity change was from January 1, 2012 to January 1, 2022. Hence, it was accepted that $t_3 =$ January 1, 2032, $t_E = t_2 =$ January 1, 2022, $t_1 =$ January 1, 2012, and $t_S = t_0 =$ November 28, 1970. The initial time was $t_0 = 1970$, the change period was from $t_1 = 2012$ to $t_2 = 2022$, and the forecast period was from $t_2 = 2022$ to $t_3 = 2032$. Previous studies suggested that the length of the change interval should be equal to that of the forecast period (Tiampo *et al.* 2002; Holliday *et al.* 2006). Using these input values, the regional and temporal forecasting of the strong earthquakes expected to occur in the Lake Van and surrounding regions in the intermediate term ($t_3 - t_2 = 10$ years) was produced for the period between

January 1, 2022 and January 1, 2032. The composite forecast map created by combining RI and PI maps is presented in Fig. 8c. Since the use of clear spatial and temporal relationships that are responsible for the interdependent behavior of earthquakes is the basis of these methods, aftershocks were not eliminated from the catalogue (Nanjo *et al.* 2006b). As can be seen in Fig. 8, the regions of the forecast earthquakes are more conspicuous on the composite map created by combining RI and PI maps. Employing these methods, the highest probability of large earthquake occurrence is determined in the regions of more intense earthquake activity or deeper seismic quiescence. As seen on the earthquake epicenter map presented in Fig. 2, the regions of higher seismic activity and strong earthquakes coincide with zones of the expected earthquakes indi-

cated on the RI, PI and combined forecast maps. As seen in Fig. 8c, some regions are the hotspots of $M_d \geq 5.0$ earthquake occurrences forecast for the 2022–2032 period. These regions are located in and around Bulanık, in the southern part of the Lake Van region including Gevaş and the adjacent regions, in the eastern part of Lake Van covering some parts of the Erciş fault, in Muradiye, Çaldıran, Van, Erçek provinces covering the Yeniköşk fault, and zones of the Van and Saray fault zones. Hence, the use of these alterna-

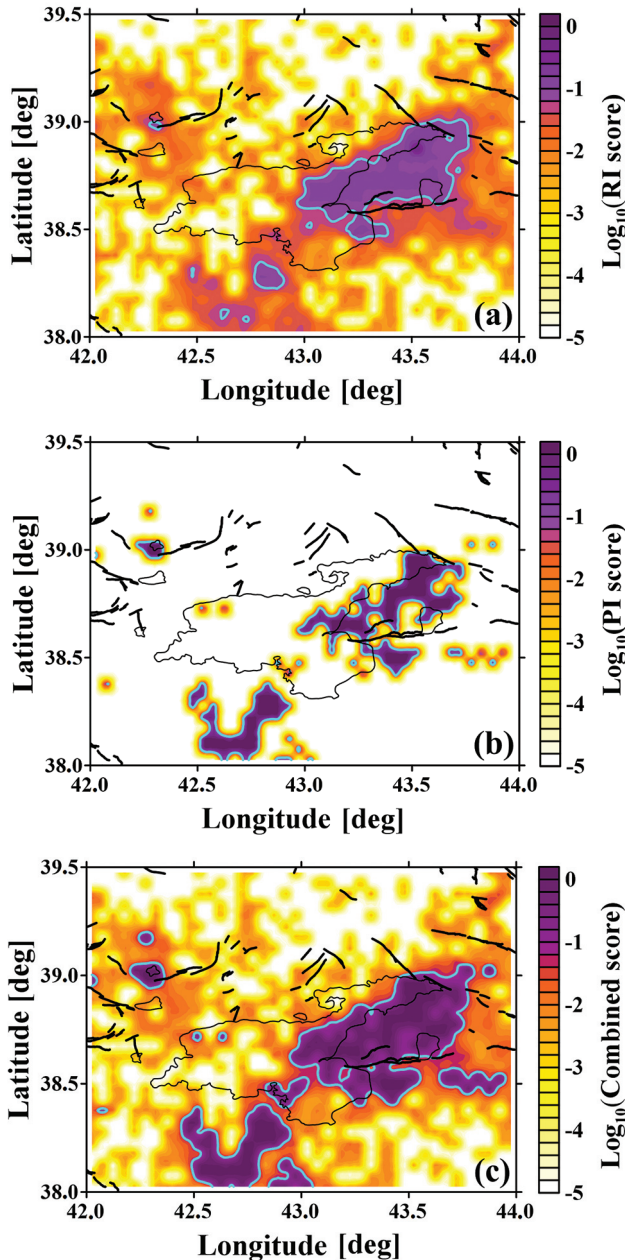


Fig. 8. (a) Forecast map created using the relative intensity method. (b) Forecast map created using the pattern informatics method; and (c) Forecast map created using the composite method. The times used are $t_0 = \text{Nov. 28, 1970}$, $t_1 = \text{Jan. 1, 2012}$, $t_2 = \text{Jan. 1, 2022}$ and $t_3 = \text{Jan. 1, 2032}$. PI score, RI score, and the combined score were presented as logarithmic values using the color code

tive methods is aimed at providing the medium-term forecasting of forthcoming earthquakes and accurately predicting the most probable time and location of their occurrence.

Coulomb stress variations at depths of 10, 20, and 30 km are represented on the maps using a grid size of 0.1×0.1 km (Fig. 9). Stress reduction and increment are represented in blue and red, respectively. As shown in Fig. 9, at a depth of 10 km, there are two positive-stress zones along the NW-SE direction and two negative-stress zones along the NE-SW one. The map for the 20 km depth is a bit of a complex structure. In summary, in the region between Van and Özalp cities, the load of stress at this depth is on the increase. As evidenced by the hypo-central distribution of events (Figs 2 and 3), this stress change originates from the Van fault zone. Stress variations at a depth of 30 km indicate positive lobes in the E-W direction and a negative-stress corridor in the N-S direction intersecting them. As evident from the map, Coulomb stress change cannot be transferred to the western part of Lake Van at all depths. Coulomb stress variation maps indicate that the eastern part of Lake Van, the Erciş fault, and the Saray fault zone are high-stress zones at all depths. Another significant zone is around Çaldıran province where mostly negative-stress change was recorded at depths of 10, 20, and 30 km. As for the earthquake epicenter distribution shown in Fig. 2, there have been no devastating earthquakes recorded in this fault zone since the 1976 earthquake. Overall, it can be stated that the recent seismic activity (2011) has been followed by small and large events in positive stress regions in the NE-SW direction.

As explained above, in some parts of the study region there are several anomaly regions showing low b -values, great Z -values, hotspot points, and positive-stress distributions. Low b -values along with high Z -values were recorded along the Çaldıran fault, in the Saray fault zone (region C), Yeniköşk fault, Van fault zone (region D), and in the southern part of Lake Van (region E). Low b -values and positive-stress changes were recorded in Muradiye-Özalp-Erçek-Van-Gevaş provinces including the northeastern part of Lake Van. Low b -values and the forecast hotspot regions are found in Çaldıran-Özalp-Erçek-Van-Muradiye provinces covering the Erciş and Yeniköşk faults as well as in zones located along the Van and Saray faults. Positive-stress distribution and forecast hotspot regions were recorded in Muradiye, Özalp, Erçek, Van, and Gevaş provinces covering the Erciş and Yeniköşk faults, and in zones along the Van and Saray faults. Also, high Z -values and forecast hotspot values were estimated for Malazgirt and Bulanık provinces (region A), in Muradiye, Çaldıran, and Özalp provinces (region C), in Van and Erçek provinces (region D), and in the southern part of Lake Van (region E). The

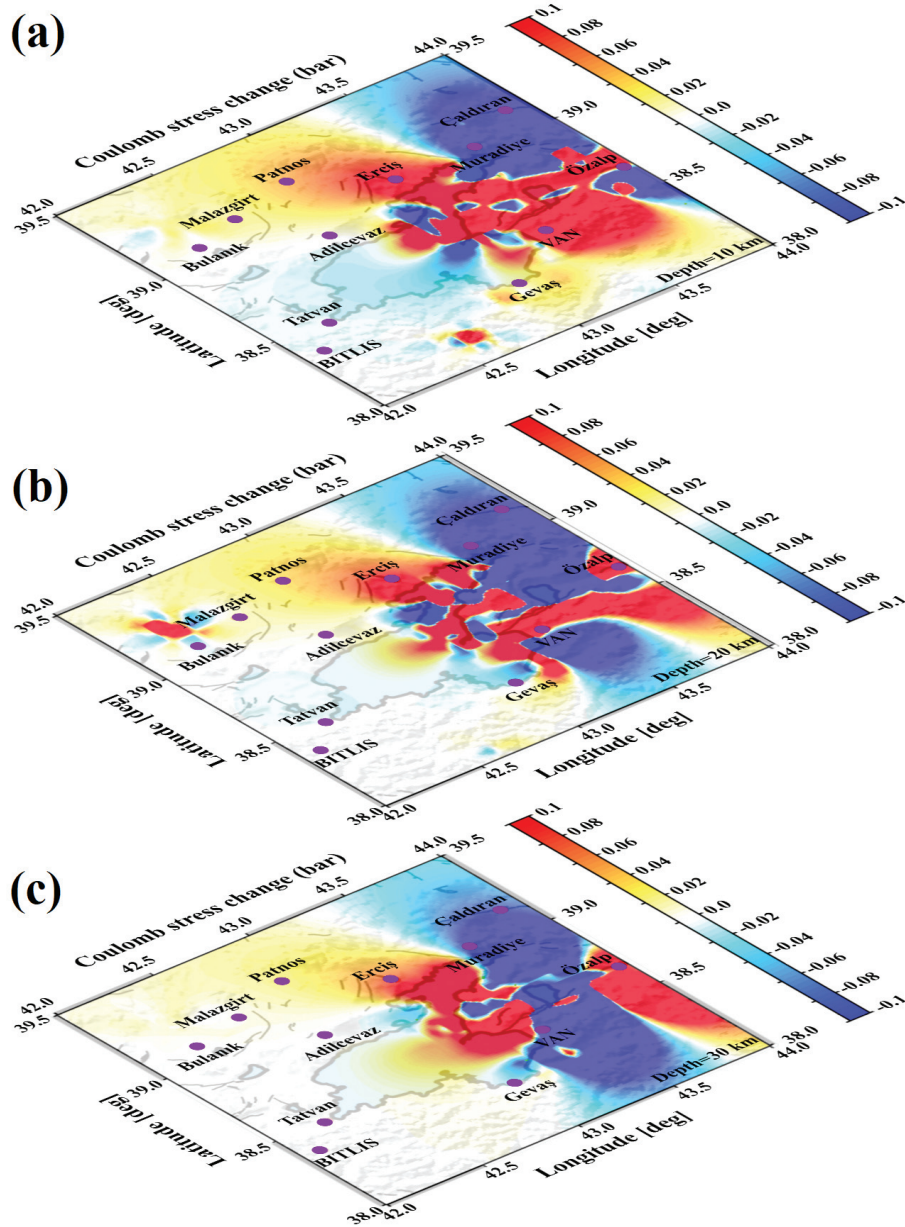


Fig. 9 Coulomb stress changes produced using the focal mechanism solutions of events listed in Table 1 at different depths: (a) 10 km, (b) 20 km, and (c) 30 km for the Lake Van region

recorded lower b -values are viewed as evidence for the high stress release and the lowest b -values may be interpreted as a sign of high strain due to the active tectonics of the study region. The low b -values may be also related to the temporal stress increase, which is released through events that are less frequent but larger in magnitude (Öncel, Wilson 2007). As mentioned in previous studies, low b -values and high-stress regions signal locations of forthcoming, potential earthquakes. The regions with lower b -values and higher Z -values may be the most probable locations of the forthcoming great earthquake occurrences. This assumption is supported by the evidenced existence of a direct relationship between a decrease in the b -value and an increase in stress values. The forecast

earthquake map created based on the analysis of spatial-temporal patterns of past earthquake events also indicates potential locations of the future earthquakes with $M_d \geq 5.0$ that are expected to occur between 2022 and 2032. As a remarkable fact, all the anomaly regions of the estimated parameters were recorded in the same regions. Therefore, these regions should receive particular attention.

DISCUSSION

Different seismotectonic parameters of earthquake occurrences in the Lake Van region have been addressed in numerous statistical studies. Comprehensive assessments of seismic, tectonic, structural,

morphological, and volcanic parameters based on the correlation between different geophysical data have been provided by numerous researchers (Utkucu 2006; Selçuk *et al.* 2010; Inan *et al.* 2012; Irmak *et al.* 2012; Kalafat *et al.* 2014; Dogan *et al.* 2014; Demirkesen, Evrendilek 2017; Öztürk 2018; Akkaya, Özvan 2019; Toker *et al.* 2021; Alkan, Bayrak 2022). Their study results indicate that the Lake Van region falls into a high-level earthquake hazard zone as regards potential intermediate- and long-term occurrences of strong earthquakes. Although this part of the EAR has been investigated in numerous different studies, statistical studies aimed to forecast earthquake occurrences in this region are relatively few. Therefore, the objective of the currently undertaken study was to perform a comprehensive spatial-temporal analysis of seismic activity aimed at assessing the earthquake potential and producing intermediate-term earthquake forecasts for this region.

Inferences about water level variation as one of the triggers of earthquakes with magnitude $M \geq 4.0$ in the Lake Van were made in a study by Utkucu (2006). The recent water level changes are claimed to be climate change-related. Study results showing temporal interrelations between earthquake activity and water level changes support the hypothesis on the hydrogeological mechanism underlying earthquake triggering. Fourteen $M \geq 5.0$ earthquakes and the increasing number of $4.0 \leq M < 5.0$ earthquake events are claimed to have been accompanied or followed by clear variations in the annual average of water level. In addition, a tendency was observed for $M \geq 4.0$ events to occur if low water levels persist throughout a year. For this reason, the monitoring of variations (increases and decreases) in the annual average of water level in combination with the earthquakes triggered by hydrogeological factors in the Lake Van region may be efficient at providing persuasive implications for the earthquake and earthquake hazard forecasting and assessment.

Selçuk *et al.* (2010) performed a probabilistic earthquake hazard assessment for the Lake Van basin applying a probabilistic approach and using the earthquake database for the 1907–2010 period. The return periods of $M_s \geq 4.0$ (M_s : surface wave magnitude) earthquakes were used to estimate the G-R parameters for the study region. Also, iso-acceleration maps of the basin were produced for the 100- and 475-year recurrence intervals. On the hazard map, the highest seismic hazard levels were determined in the northeastern, northwestern, and southwestern parts of Lake Van, within the Lake and its shores. Thus, the findings and relations between seismotectonic earthquake parameters in our study are very similar to those reported by Selçuk *et al.* (2010). These results indicate that serious earthquake hazards may be expected in

the above-mentioned parts of the study region in the intermediate/long term.

Inan *et al.* (2012) performed a chemical analysis of the bottled spring water gushing out from the 2011 Van earthquake epicenter location, which revealed clear increases in Ca^{2+} , Mg^{2+} , K^+ , and Cl^- contents, and decreases in Na^+ and SO_4^{2-} contents. As reported by the authors, all ion concentrations stabilized nearly a month after the main shock. Hence, it was hypothesized that chemical spring water anomalies may be considered as potential geochemical pre-earthquake precursors. To reveal the mechanisms responsible for the reported pre-earthquake geochemical anomalies, these regions must be subjected to multi-disciplinary, i.e., seismological, geodetical, or geochemical, observation. Thus, the observation of recent variations (decreases and increases) in these types of parameters and their assessment together with our results may be highly promising for providing preliminary indicators of seismic hazard in the Lake Van region.

The rupture process of the 2011 Van earthquake and aftershocks with their tectonic implications were analyzed by Irmak *et al.* (2012). They compared the fault-plane solutions with the surface rupture geometry for active tectonics modeling in the region. Their results showed that the Van earthquake occurred on the main thrust fault plane trending northeast-southwest between Lakes Van and Erçek located in the East Anatolian compressional province. Analysis of the total slip distribution showed that a great asperity region could be seen with a large slip in and around the hypo-central region. As stated by the researchers, the rupture was very smooth and gradually expanded near the hypocenter and propagated bilaterally in northeastern and mainly southwestern directions. Hence, the results obtained by Irmak *et al.* (2012) support the results of our study.

Kalafat *et al.* (2014) analyzed the fault-plane solutions of the 2011 Van earthquake and its aftershocks to define the deformation and stress regime in the Lake Van region. The distribution of strong earthquake events and aftershocks proved that seismicity in the region was caused by faults trending east-west and northeast-southwest. According to the results of focal mechanism and stress analysis solutions for the 2011 Van earthquake, events occurred on the reverse faulting and the earthquake activity in the study area continued in the compressional regime. The authors concluded that the Van earthquake caused the regional stress distribution, which triggered earthquakes on adjacent faults. Later, mid-sized events can be expected to occur on the nearby faults due to the apparent stress drop on the fault related to the mainshock. It is a remarkable fact that the results and the relationships between seismotectonic parameters calculated in our study are compatible with those reported by Kalafat *et al.* (2014).

Dogan *et al.* (2014) investigated spatial-temporal patterns of the post-seismic deformation that took place after the 2011 Van earthquake to obtain evidence for the aseismic fault reactivation. They analyzed the geodetic parameters after the 2011 Van earthquake and revealed a fault splay on the footwall block of the co-seismic thrust fault. According to their results, the slip deficit on the shallow part of the co-seismic fault determined by interferometric synthetic aperture radar-based models was partially filled by an aseismic slip. They stated that stress transfer due to aseismic slip could also be taken into consideration when evaluating earthquake hazards on the adjacent seismically active faults. Evaluation of stress changes due to co-seismic and post-seismic slips on the Van rupture using various seismotectonic parameters considered in this study may be a more accurate approach to earthquake forecasting in the study region.

According to Demirkesen, Evrendilek (2017), in terms of earthquake vulnerability, and pre-earthquake preparedness, the Lake Van region has not been researched sufficiently. Therefore, these researchers provided the digital description of the Lake Van region relief and its interpretation in terms of the potential earthquake potential, using remote sensing systems in combination with geographical information. Their results revealed that Erciş-Van-Gevaş-Tatvan provinces face the highest earthquake risk, and these results are compatible with those obtained in the current study. Thus, the spatial-temporal mapping and monitoring of different geophysical, geological, or geodetic parameters may provide more reliable interpretations for assessing and forecasting earthquake hazards, which, in their turn, would allow avoiding structural failure and taking emergency preparedness measures to minimize pain and loss of life caused by major earthquake disasters.

Öztürk (2018) conducted the region-time-magnitude analysis of the seismic activity in the EAR based on the b - D_c -, and Z -values. In this study, the regions with high Z -values and small b -values were considered as the most likely regions for the forthcoming earthquake occurrences. Öztürk (2018) demonstrated that correlations between these seismic and tectonic parameters can provide important evidence about the seismic hazard situation and be used as a significant tool for earthquake forecasting. In the present study, some anomaly regions were found to have low b -values, high Z -values, high-stress distribution, and hotspot scores. Thus, the anomaly regions such as Van, Muradiye, Çaldıran, Özalp, Erçek, and Gevaş provinces including Erciş, Çaldıran, and Yeniköşk faults as well as the fault zone of Van and Saray must be given particular attention.

Akkaya, Özvan (2019) investigated the site characteristics of the Van settlement using surface waves and

the horizontal-to-vertical spectral ratio microtremor method. According to these researchers, it is a region of active tectonism and numerous large earthquake events. For this reason, the site effect plays an important role in assessing earthquake damage and designing new structures. Hence, these researchers aimed to determine the physical and mechanical characteristics of soils in the Van settlement and adjacent regions and to describe their behavior during a potential earthquake. As has been explained already, the region under study is located on generally young, unconsolidated, and saturated, current lake and stream sediments. According to these authors, the eastern part of Lake Van has still a high potential to generate strong earthquakes. The results of the performed multiple parameter analysis and the site properties determined in the study by Akkaya, Özvan (2019) are highly useful in earthquake forecasting and evaluating quality deficiencies of structures in the Lake Van region.

Toker *et al.* (2021) performed an integrated analysis of the October 23, 2011 Van earthquake by estimating Coulomb stress variations for the off-fault aftershocks. They presumed that the local source of lateral changes in stress distributions in crustal and sub-crustal structures strongly disturbs the regional stress field. They hypothesized that the strike-slip motion was generated by sub-crustal ductile processes in the absence of the mantle lid. According to Toker *et al.* (2021), their analyses provide new perspective for the significant role of stress accumulation under the Lake Van and Erçek areas. They arrived at a conclusion that the evaluation of stress limits facilitates the determination of the off-fault seismicity triggered by stress transfer and forecast earthquake hazards. For this reason, these types of studies should be supported by different statistical earthquake parameters as is the case in our study. Thus, the assessment of the intermediate/long term seismic hazard potential in the study region must be comprehensive.

In their study, Alkan, Bayrak (2022) aimed to evaluate the seismic potential in the Lake Van region based on the analysis of the tectonic stress variation performed using the so-called method of the Coulomb stress change and the b -value distribution. To that end, the above-mentioned authors performed the Coulomb stress analysis of 83 local events that occurred between 2000 and 2020 and calculated the b -values for 17,815 events that occurred between 1903 and 2021. Their findings (low b -values and positive Coulomb stress changes) show that Van, Yenişehir, Başkale and Çaldıran faults have a high seismic potential in the future. The results reported by Alkan, Bayrak (2022) are in corroboration with those obtained in this study.

The performed literature survey and the findings of the present study prove that a comprehensive as-

assessment of the seismotectonic parameters such as the b -value, Z -value, the hotspot points determined applying RI and PI methods, and the Coulomb stress change provide more reliable evidence for the reliable assessment and forecasting of seismic hazards in the Lake Van region. This region was struck by strong earthquakes in the past and many moderate earthquakes have occurred in and around Lake Van in recent years. Therefore, future earthquake forecasting in this region is of critical importance. The types of seismic hazard assessments discussed in this study should be based on the monitoring and/or analysis of multiple geophysical parameters. As for the data and parameters used in this study, the above-mentioned anomaly regions, and the obtained results such as the low b -value, high Z -value, hotspot points, and high-stress distributions, are supported by other geophysical parameters. Consequently, these regions must be given particular attention, and the analysis of spatial-temporal correlations among different seismotectonic parameters can prove efficient in seismic hazard assessment and large earthquake forecasting in and around the Lake Van region in the intermediate term.

CONCLUSIONS

The seismotectonic b -value, precursory seismic quiescence Z -value, RI and PI algorithms, and Coulomb stress changes were evaluated in this study for assessing and forecasting earthquake hazards in the Lake Van region of Turkey. For these analyses, we used a homogeneous earthquake catalogue including 14,178 shallow events (depth < 70 km) with the magnitude of $1.0 \leq M_d \leq 6.6$, which occurred from November 28, 1970 to December 31, 2021. We performed our analyses in a rectangular study area within the coordinates $38.0^\circ\text{N} - 39.5^\circ\text{N}$ and $42.0^\circ\text{E} - 44.0^\circ\text{E}$. Sixty-six seismic events with the magnitude of $M_w \geq 4.5$ recorded in and around the Lake Van region between 2011 and 2021 were used for the mapping of Coulomb stress changes. Firstly, spatial, and temporal patterns of earthquake behavior were mapped using b - and Z -values, after which the analysis of the Coulomb stress variation recorded at the beginning of 2022 was performed. Then the forecast of future strong earthquake occurrences was made by superimposing RI and PI scores for the time interval of 2022–2032. It should be emphasized that for the forecasting of strong earthquakes in this region of Turkey, these techniques were employed for the first time.

The anomaly regions exhibiting small b -values, high Z -values, hotspot points determined from combined forecast maps, and positive Coulomb stress changes include Muradiye, Çaldıran, Özalp, Erçek, Van city center, and Gevaş provinces, covering the

faults of Çaldıran, Yeniköşk, Erciş, and Malazgirt as well as the fault zones of Saray and Van. The regions showing small b -values, high Z -values, and positive-stress distribution are considered to be the most potential locations of the expected strong earthquake occurrences. The forecast of the forthcoming $M_d \geq 5.0$ earthquakes that are expected to occur between 2022 and 2032 shows that locations of the predicted earthquakes coincide with the anomaly regions determined based on the analysis results of various seismotectonic parameters. Our results indicate that the correlation existing between these variables contributes to a better understanding of seismic, tectonic, and structural properties of the region.

From the above findings, it can be concluded that a more promising strategy for the forecasting of the time and location of the forthcoming potential earthquakes should be based on the comprehensive analysis of multiple parameters. This conclusion is confirmed by the correlations among all the estimated parameters that can be considered among the indicators of strong earthquakes. Thus, the present study demonstrates that multiple parameter analysis may prove efficient for the intermediate-term earthquake forecasting in the Lake Van region.

ACKNOWLEDGMENTS

Some images were obtained from ZMAP and GMT package programs (Wiemer 2001; Wessel *et al.* 2019). The maps of Coulomb stress changes were created using the Coulomb 3.4 package (Toda *et al.* 2011). Tectonic units were taken from Emre *et al.* (2013, 2018). The authors would like to thank Dr. Kazuyoshi Z. Nanjo for helping with the preparation of RI, PI, and combined codes. Earthquake catalogues for the period 1970–2006 are available at Öztürk (2009). Data on the earthquake occurrences in the period 2006–2022 were obtained from Bogazici University, Kandilli Observatory and Research Institute (KOERI, www.koeri.boun.edu.tr/sismo/zeqdb/). The catalogue information (dip, strike, rake, etc.) relating to focal mechanisms of earthquakes was provided by the Disaster and Emergency Management Authority (AFAD, www.afad.gov.tr). The authors would like to thank anonymous reviewers for their useful and constructive suggestions that have improved this paper, and the Editor-in-Chief for his editorial suggestions.

REFERENCES

- Abdelfattah, A.K., Jallouli, C., Qaysi, S., Al-Qadasi, B. 2020. Crustal stress in the Northern Red Sea region as inferred from seismic b -values, seismic moment release, focal mechanisms, gravity, magnetic, and heat flow data. *Surveys in Geophysics* 41, 963–986. <https://doi.org/10.1007/s10712-020-09602-8>

- Ahadov, B., Jin, S. 2019. Effects of Coulomb stress change on $M_w > 6$ earthquakes in the Caucasus region. *Physics of the Earth and Planetary Interiors* 29 (106326), 1–12. <https://doi.org/10.1016/j.pepi.2019.106326>
- Akkaya, İ., Özvan, A. 2019. Site characterization in the Van settlement (Eastern Turkey) using surface waves and HVSr microtremor methods. *Journal of Applied Geophysics* 160, 157–170. <https://doi.org/10.1016/j.jappgeo.2018.11.009>
- Alkan, H., Bayrak, E. 2022. Coulomb stress change and magnitude-frequency distribution for Lake Van region. *Bulletin of the Mineral Research and Exploration* 168, 141–156. <https://doi.org/10.19111/bulletinofmre.990666>
- Alkan, H., Çınar, H., Oreshin, S. 2020. Lake Van (south-eastern Turkey) experiment: Receiver function analyses of lithospheric structure from teleseismic observations. *Pure and Applied Geophysics* 177, 3891–3909. <https://doi.org/10.1007/s00024-020-02447-7>
- Alkan, H., Büyüksaraç, A., Bektaş, Ö., Işık, E. 2021. Coulomb stress change before and after 24.01.2020 Sivrice (Elazığ) Earthquake ($M_w = 6.8$) on the East Anatolian Fault Zone. *Arabian Journal of Geosciences* 14, 2648. <https://doi.org/10.1007/s12517-021-09080-1>
- Bayrak, Y., Öztürk, S., Çınar, H., Kalafat, D., Tsapanos, T.M., Koravos, G.Ch., Leventakis, G.A., 2009. Estimating earthquake hazard parameters from instrumental data for different regions in and around Turkey. *Engineering Geology* 10, 200–210.
- Beroza, C.G., Segou, M., Mousavi, M. 2021. Machine learning and earthquake forecasting-next steps. *Nature Communications* 12 (4761), 1–3. <https://doi.org/10.1038/s41467-021-24952-6>
- Bowman, D.D., King, G.C.P. 2001. Accelerating seismicity and stress accumulation before large earthquakes. *Geophysical Research Letters* 28, 4039–4042. <https://doi.org/10.1029/2001GL013022>
- Bozkurt, E. 2001. Neotectonics of Turkey – a synthesis. *Geodinamica Acta* 14, 3–30. [https://doi.org/10.1016/S0985-3111\(01\)01066-X](https://doi.org/10.1016/S0985-3111(01)01066-X)
- Console, R., Montuori, C., Murru, M. 2000. Statistical assessment of seismicity patterns in Italy: Are they precursors of subsequent events?. *Journal of Seismology* 4, 435–449. <https://doi.org/10.1023/A:1026540018598>
- Çukur, D., Krastel, S., Tomonaga, Y., Schmincke, H.U., Sumita, M., Meydan, A.F., Çağatay, M.N., Toker, M., Kim, S.P., Kong, G.S., Horozal, S. 2017. Structural characteristics of the Lake Van Basin, eastern Turkey, from high-resolution seismic reflection profiles and multibeam echosounder data: geologic and tectonic implications. *International Journal of Earth Sciences (Geol. Rundsch)* 106, 239–253. <https://doi.org/10.1007/s00531-016-1312-5>
- Demirkesen, A.C., Evrendilek, F. 2017. Digital terrain characterization and interpretation of Lake Van region for earthquake vulnerability combining remote sensing and geographical information systems. *Fresenius Environmental Bulletin* 26(2a), 1745–1755.
- Derode, B., Madariaga, R., Campos, J. 2021. Seismic rate variations prior to the 2010 Maule, Chile M_w 8.8 giant megathrust earthquake. *Nature* 11 (2705), 1–9. <https://doi.org/10.1038/s41598-021-82152-0>
- Dogan, U., Demir, D.O., Çakir, Z., Ergintav, S., Ozener, H., Akoğlu, A.M., Nalbant, S.S., Reilinger, R. 2014. Post-seismic deformation following the M_w 7.2, 23 October 2011 Van earthquake (Turkey): Evidence for aseismic fault reactivation. *Geophysical Research Letters* 41, 2334–2341. <https://doi.org/10.1002/2014GL059291>
- Emre, O., Duman, T.Y., Ozalp, S., Elmaci, H., Olgun, S., Saroglu, F. 2013. 1/1.125.000 scale
- Emre, Ö., Duman, T.Y., Özalp, S., Şaroğlu, F., Olgun, Ş., Elmaci, H., Çan, T. 2018. Active fault database of Turkey. *Bulletin of Earthquake Engineering* 16, 3229–3275. <https://doi.org/10.1007/s10518-016-0041-2>
- Enescu, B., Ito, K. 2002. Spatial analysis of the frequency-magnitude distribution and decay rate of aftershock activity of the 2000 Western Tottori earthquake. *Earth Planets and Space* 54, 847–859. <https://doi.org/10.1186/BF03352077>
- Frohlich, C., Davis, S. 1993. Teleseismic b -values: Or, much ado about 1.0. *Journal of Geophysical Research* 98 (B1), 631–644. <https://doi.org/10.1029/92JB01891>
- Gutenberg, R., Richter, C.F. 1944. Frequency of earthquakes in California. *Bulletin of the Seismological Society of America* 34, 185–188. <https://doi.org/10.1038/156371a0>
- Gülüüz, E., Durak, H., Özkaptan, M., Krijgsman, W. 2020. Paleomagnetic constraints on the early Miocene closure of the southern NeoTethys (Van region; East Anatolia): Inferences for the timing of Eurasia Arabia Collision. *Global and Planetary Change* 185 (103089), 1–13. <https://doi.org/10.1016/j.gloplacha.2019.103089>
- Holliday, J.R., Nanjo, K.Z., Tiampo, K.F., Rundle, J.B., Turcotte, D.L. 2005. Earthquake forecasting and its verification. *Nonlinear Processes in Geophysics* 12, 965–977. <https://doi.org/10.5194/npg-12-965-2005>
- Holliday, J.R., Rundle, J.B., Tiampo, K.F., Turcotte, D.L. 2006. Using earthquake intensities to forecast earthquake occurrence time. *Nonlinear Processes in Geophysics* 13, 585–593. <https://doi.org/10.5194/npg-13-585-2006>
- Holliday, J.R., Chen, C-C., Tiampo, K.F., Rundle, J.B., Turcotte, D.L., Donnellan, A. 2007. A RELM earthquake forecast based on Pattern Informatics. *Seismological Research Letters* 78 (1), 87–93. <https://doi.org/10.1785/gssrl.78.1.87>
- Huang, Q., Sobolev, G.A., Nagao, T. 2001. Characteristics of the seismic quiescence and activation patterns before the $M = 7.2$ Kobe earthquake, January 17, 1995. *Tectonophysics* 337, 99–116. [https://doi.org/10.1016/S0040-1951\(01\)00073-7](https://doi.org/10.1016/S0040-1951(01)00073-7)
- Inan, S., Balderer, W.P., Leuenberger-West, F., Yakan, H., Özvan, A., Freund, F.T. 2012. Springwater chemical anomalies prior to $M_w = 7.2$ Van earthquake (Turkey). *Geochemical Journal* 46 (1), 11–16. <https://doi.org/10.2343/geochemj.1.0159>
- Irmak, T.S., Dogan, B., Karakas, A. 2012. Source mech-

- anism of the 23 October 2011, Van (Turkey) earthquake (Mw = 7.1) and aftershocks with its tectonic implications. *Earth Planets and Space* 64, 991–1003. <https://doi.org/10.5047/eps.2012.05.002>
- Joseph, J.D.R., Rao, B., Anoop, M.B. 2011. A study on clustered and de-clustered world-wide earthquake data using G-R recurrence law. *International Journal of Earth Science and Engineering* 4, 178–182.
- Kalafat, D., Kekovalı, K., Akkoyunlu, F., Ögütçü, Z. 2014. Source mechanism and stress analysis of 23 October 2011 Van Earthquake (Mw = 7.1) and aftershocks. *Journal of Seismology* 18, 371–384. <https://doi.org/10.1007/s10950-013-9413-0>
- Katsumata, K., Kasahara, M. 1999. Precursory seismic quiescence before the 1994 Kurile earthquake (Mw = 8.3) revealed by three independent seismic catalogs. *Pure and Applied Geophysics* 155, 43–470. <https://doi.org/10.1007/s000240050274>
- Kayın, S., İşseven, T. 2023. New paleomagnetic results from Neogene to Quaternary volcanic rocks of north of the Lake Van, Eastern Turkey. *Scientific Reports* 13 (12206), 1–17. <https://doi.org/10.1038/s41598-023-39492-w>
- Keilis-Borok, VI. 1996. Intermediate term earthquake prediction. *Proceedings of the National Academy of Sciences, USA* 93, 3748–3755. <https://doi.org/10.1073/pnas.93.9.3748>
- Keilis-Borok, VI., Soloviev, A.A. 2003. *Nonlinear dynamics of the lithosphere and earthquake prediction. Physics-Multi-Author Volume "Topical Volume"*. Editorial W. Beiglböck. Springer-Verlag Berlin Heidelberg, New York. XIII:337
- Keskin, M. 2003. Magma generation by slab steepening and breakoff beneath a subduction–accretion complex: an alternative model for collision-related volcanism in Eastern Anatolia, Turkey. *Geophysical Research Letters* 30 (24), 8046. <https://doi.org/10.1029/2003GL018019>
- King, G.C., Stein, R.S., Lin, J. 1994. Static stress changes and the triggering of earthquakes. *Bulletin of the Seismological Society of America* 84 (3), 935–953. <https://doi.org/10.1785/BSSA0840030935>
- Li, Y., Chen, X. 2021. Variations in apparent stress and *b* value preceding the 2010 Mw8.8 Bio-Bío, Chile. *Pure and Applied Geophysics* 178, 4797–4813. <https://doi.org/10.1007/s00024-020-02637-3>
- Liao, B.Y., Huang, H.C., Xie, S. 2022. The source characteristics of the M 6.4, 2016 Meinong Taiwan earthquake from teleseismic data using the hybrid homomorphic Deconvolution method. *Applied Sciences* 12 (494), 1–13. <https://doi.org/10.3390/app12010494>
- Luginbuhl, M., Rundle, J.B., Turcotte, D.L. 2018. Statistical physics models for aftershocks and induced seismicity. *Philosophical Transactions of the Royal Society A* 337, 20170397. <https://doi.org/10.1098/rsta.2017.0397>
- McClusky, S., Balassanian, S., Barka, A., Demir, C., Ergintav, S., Georgiev, I., Gurkan, O., Hamburger, M., Hurst, K., Kahle, H., Kastens, K., Kekelidze, G., King, R., Kotzev, V., Lenk, O., Mahmoud, S., Mishin, A., Nadariya, M., Ouzounis, A., Paradissis, D., Peter, Y., Prilepin, M., Reilinger, R., Sanli, I., Seeger, H., Tealeb, A., Toksöz, M.N., Veis, G. 2000. GPS constraints on plate motions and deformation in the Eastern Mediterranean: implications for plate dynamics. *Journal Geophysical Research* 105, 5695–5719. <https://doi.org/10.1029/1996JB900351>
- Mizrahi, L., Nandan, S., Wiemer, S. 2021. The effect of declustering on the size distribution of mainshocks. *Seismological Research Letters* 92 (4), 2333–2342. <https://doi.org/10.1785/0220200231>
- Mogi, K. 1962. Magnitude-frequency relation for elastic shocks accompanying fractures of various materials and some related problems in earthquakes. *Bulletin of the Earthquake Research Institute, Tokyo University* 40, 831–853.
- Nalbant, S.S., McCloskey, J., Steacy, S., Barka, A.A. 2002. Stress accumulation and increased seismic risk in Eastern Turkey. *Earth and Planetary Science Letters* 195 (3–4), 291–298. [https://doi.org/10.1016/S0012-821X\(01\)00592-1](https://doi.org/10.1016/S0012-821X(01)00592-1)
- Nanjo, K.Z. 2020. Were changes in stress state responsible for the 2019 Ridgecrest, California, earthquakes? *Nature Communication* 11 (3082), 1–10. <https://doi.org/10.1038/s41467-020-16867-5>
- Nanjo, K.Z., Rundle, J.B., Holliday, J.R., Turcotte, D.L. 2006a. Pattern Informatics and its application for optimal forecasting of large earthquakes in Japan. *Pure and Applied Geophysics* 163, 2417–2432. <https://doi.org/10.1007/s00024-006-0130-2>
- Nanjo, K.Z., Holliday, J.R., Chen, C.-c., Rundle, J.B., Turcotte, D.L. 2006b. Application of modified pattern informatics method to forecasting the locations of future large earthquakes in the central Japan. *Tectonophysics* 424, 351–366. <https://doi.org/10.1016/j.tecto.2006.03.043>
- Okada, Y. 1985. Surface deformation due to shear and tensile faults in a half-space. *Bulletin of the Seismological Society of America* 75 (4), 1135–1154. <https://doi.org/10.1785/BSSA0750041135>
- Olsson, R. 1999. An estimation of the maximum *b*-value in the Gutenberg-Richter relation. *Journal of Geodynamics* 27 (4), 547–55. [https://doi.org/10.1016/S0264-3707\(98\)00022-2](https://doi.org/10.1016/S0264-3707(98)00022-2)
- Ozer, C., Polat, O. 2017. 3-D crustal velocity structure of Izmir and surroundings. *Journal of the Faculty of Engineering and Architecture of Gazi University* 32 (3), 733–747. <https://doi.org/10.17341/gazimmfd.337620>
- Öncel, A.O., Wilson, T.H. 2007. Anomalous seismicity preceding the 1999 Izmit event, NW Turkey. *Geophysical Journal International* 169 (1), 259–270. <https://doi.org/10.1111/j.1365-246X.2006.03298.x>
- Öztürk, S. 2009. An application of the earthquake hazard and aftershock probability evaluation methods to Turkey earthquakes. PhD Thesis, Karadeniz Technical University, Trabzon, Turkey (in Turkish with English abstract), pp 346.
- Öztürk, S. 2011. Characteristics of seismic activ-

- ity in the western, central and eastern parts of the North Anatolian Fault Zone, Turkey: temporal and spatial analysis. *Acta Geophysica* 59, 209–238. <https://doi.org/10.2478/s11600-010-0050-5>
- Öztürk, S. 2017. Space-time assessing of the earthquake potential in recent years in the eastern Anatolia region of Turkey. *Earth Sciences Research Journal* 21 (2), 67–75. <https://doi.org/10.15446/esrj.v21n2.50889>
- Öztürk, S. 2018. Earthquake hazard potential in the Eastern Anatolian region of Turkey: seismotectonic b and D_c -values and precursory quiescence Z -value. *Frontiers of Earth Sciences* 12 (1), 215–236. <https://doi.org/10.1007/s11707-017-0642-3>
- Öztürk, S. 2020. A study on the variations of recent seismicity in and around the Central Anatolian region of Turkey. *Physics of the Earth and Planetary Interiors* 301 (106453), 1–11. <https://doi.org/10.1016/j.pepi.2020.106453>
- Öztürk, S., Alkan, H. 2022a. A statistical analysis and evaluation on the earthquake forecasting and hazard for the Lake Van and its adjacent area (Turkey). *Türk Deprem Araştırma Dergisi* 4 (2), 191–209.
- Öztürk, S., Alkan, H. 2022b. A Study on the earthquake hazard and forecasting in the Lake Van and its surroundings, Turkey. *International Conference on Mathematics: An Istanbul Meeting for World Mathematicians, ICOM-2022*. Istanbul, Turkey.
- Polat, O., Eyidoğan, H., Haessler, H., Cisternas, A., Philip, H. 2002. Analysis and interpretation of the aftershock sequence of the August 17, 1999, Izmit (Turkey) earthquake. *Journal of Seismology* 6, 287–306. <https://doi.org/10.1023/A:1020075106875>
- Puangjaktha, P., Pailoplee, P. 2018. Temporal and spatial distributions of precursory seismicity rate changes in the Thailand-Laos-Myanmar border region: implication for upcoming hazardous earthquakes. *Journal of Seismology* 22, 303–313. <https://doi.org/10.1007/s10950-017-9706-9>
- Reasenber, P.A. 1985. Second-order moment of Central California seismicity, 1969–1982. *Journal of Geophysical Research* 90 (B7), 5479–5495. <https://doi.org/10.1029/JB090iB07p05479>
- Reilinger, R., McClusky, S., Vernant, P., Lawrence, S., Ergintav, S., Cakmak, R. 2006. GPS constraints on continental deformation in the Africa-Arabia-Eurasia continental collision zone and implications for the dynamics of plate interactions. *Journal of Geophysical Research* 111 (B05411), 1–26. <https://doi.org/10.1029/2005JB004051>
- Rundle, J.B., Tiampo, K.F., Klein, W., Martins, J.S.S. 2002. Self-organization in leaky threshold systems: The influence of near-mean field Dynamics and its implications for earthquakes, neurobiology and forecasting. *Proceedings of the National Academy of Sciences, USA* 99 (Supplement 1), 2514–2521. <https://doi.org/10.1073/pnas.012581899>
- Scholz, C.H. 2015. On the stress dependence of the earthquake b value. *Geophysical Research Letters* 42, 1399–1402. <https://doi.org/10.1002/2014GL062863>
- Schorlemmer, D., Wiemer, S., Wyss, M. 2005. Variations in earthquake-size distribution across different stress regimes. *Nature* 437, 539–42. <https://doi.org/10.1038/nature04094>
- Selçuk, A.S. 2016. Evaluation of the relative tectonic activity in the eastern Lake Van basin, East Turkey. *Geomorphology* 270, 9–21. <https://doi.org/10.1016/j.geomorph.2016.07.009>
- Selçuk, L., Selçuk, A.S., Beyaz, T. 2010. Probabilistic seismic hazard assessment for Lake Van basin, Turkey. *Natural Hazards* 54, 949–965. <https://doi.org/10.1007/s11069-010-9517-6>
- Smith, W.D. 1981. The b -value as an earthquake precursor. *Nature* 289, 136–139. <https://doi.org/10.1038/289136a0>
- Sobolev, G.A., Tyupkin, Y.S. 1997. Low-seismicity precursors of large earthquakes in Kamchatka. *Volcanology and Seismology* 18 (4), 433–446. <https://doi.org/10.1134/S0742046308020036>
- Stein, R.S., King, G.C.P., Lin, J. 1994. Stress Triggering of the 1994 $M = 6.7$ Northridge, California, earthquake by its predecessors. *Science* 265 (5177), 1432–1435. <https://doi.org/10.1126/science.265.5177.1432>
- Stein, R.S., Barka, A.A., Dieterich, J.H. 1997. Progressive failure on the North Anatolian fault since 1939 by earthquake stress triggering. *Geophysical Journal International* 128, 594–604.
- Şengör, A.M.C., Ozeren, S., Genc, T., Zor, E. 2003. East Anatolian high plateau as a mantle-supported, north-south shortened domal structure. *Geophysical Research Letters* 30 (4), 8045. <https://doi.org/10.1029/2003GL017858>
- Tiampo, K.F., Rundle, J.B., McGinnis, S.A., Klein, W. 2002. Pattern dynamics and forecast methods in seismically active regions. *Pure and Applied Geophysics* 159, 2429–2467. <https://doi.org/10.1007/s00024-002-8742-7>
- Toda, S., Stein, R.S., Richards-Dinger, K., Bozkurt, S.B. 2005. Forecasting the evolution of seismicity in southern California: animations built on earthquake stress transfer. *Journal of Geophysical Research* 110, B05S16. <https://doi.org/10.1029/2004J B0034 15>
- Toda, S., Stein, R.S., Sevilgen, V., Lin, J. 2011. Coulomb 3.3 Graphic-rich deformation and stress-change software for earthquake, tectonic, and volcano research and teaching-user guide. *U.S. Geological Survey Open-File Report* 2011–1060, 63 pp., available at <https://pubs.usgs.gov/of/2011/1060/>
- Toker, M. 2021. The structural coupling to rupture complexity of the aftershock sequence of the 2011 earthquakes in Lake Van area (Eastern Anatolia, Turkey). *Journal of Engineering Design* 9 (1), 27–51. <https://doi.org/10.21923/jesd.861520>
- Toker, M., Pinar, A., Hoşkan, N. 2021. An integrated critical approach to off-fault strike-slip motion triggered by the 2011 Van mainshock (M_w 7.1), Eastern Anatolia (Turkey): New stress field constraints on subcrustal deformation. *Journal of Geodynamics* 147, 1–25. 101861. <https://doi.org/10.1016/j.jog.2021.101861>

- Turcotte, D.L. 1991. Earthquake prediction. *Annual Review of Earth Planetary Sciences* 19, 263–281.
- Ulukavak, M., Yalçinkaya, M., Kayıkçı, E.T., Öztürk, S., Kandemir, R., Karşlı, H. 2020. Analysis of ionospheric TEC anomalies for global earthquakes during 2000-2019 with respect to earthquake magnitude ($M_w \geq 6.0$). *Journal of Geodynamics* 135 (101721), 1–10. <https://doi.org/10.1016/j.jog.2020.101721>
- Utkucu, M. 2006. Implications for the water level change triggered moderate ($M \geq 4.0$) earthquakes in Lake Van basin, Eastern Turkey. *Journal of Seismology* 10, 105–117. <https://doi.org/10.1007/s10950-005-9002-y>
- Utkucu, M., Durmuş, H., Yalçın, H., Budakoğlu, E., Işık, E. 2013. Coulomb static stress changes before and after the 23 October 2011 Van, Eastern Turkey, earthquake ($M_w = 7.1$): implications for the earthquake hazard mitigation. *Natural Hazards and Earth System Sciences* 13, 1889–1902. <https://doi.org/10.5194/nhess-13-1889-2013>
- Utsu, T. 1971. Aftershock and earthquake statistic (III): Analyses of the distribution of earthquakes in magnitude, time and space with special consideration to clustering characteristics of earthquake occurrence (1). *Journal of the Faculty of Science, Hokkaido University. Series VII (Geophysics)* 3, 379–441.
- Varotsos, P., Alexopoulos, K. 1984. Physical properties of the variations of the electric field of the earth preceding earthquakes. II. determination of epicenter and magnitude. *Tectonophysics* 110, 99–125. [https://doi.org/10.1016/0040-1951\(84\)90060-X](https://doi.org/10.1016/0040-1951(84)90060-X)
- Wessel, P., Luis, J.F., Uieda, L., Scharroo, R., Wobbe, F., Smith, W.H.F., Tian, D. 2019. The Generic Mapping Tools version 6. *Geochemistry Geophysics Geosystems* 20, 5556–5564. <https://doi.org/10.1029/2019GC008515>
- Wiemer, S. 2001. A software package to analyze seismicity: ZMAP. *Seismological Research Letters* 72 (2), 373–382. <https://doi.org/10.1785/gssrl.72.3.373>
- Wiemer, S., Wyss, M. 1994. Seismic quiescence before the Landers ($M = 7.5$) and Big Bear (6.5) 1992 earthquakes. *Bulletin of the Seismological Society of America* 84 (3), 900–916. <https://doi.org/10.1785/BSSA0840030900>
- Wiemer, S., Wyss, M. 2000. Minimum magnitude of completeness in earthquake catalogs: Examples from Alaska, the Western United States, and Japan. *Bulletin of the Seismological Society of America* 90 (3), 859–869. <https://doi.org/10.1785/0119990114>
- Woessner, J., Wiemer, S. 2005. Assessing the quality of earthquake catalogues: Estimating the magnitude of completeness and its uncertainty. *Bulletin of the Seismological Society of America* 95 (2), 684–698. <https://doi.org/10.1785/0120040007>
- Wyss, M., Habermann, R.E. 1988. Precursory seismic quiescence. *Pure and Applied Geophysics* 126 (2–4), 319–332. <https://doi.org/10.1007/BF00879001>
- Yadav, R.B.S., Gahalaut, V.K., Chopra, S.B. 2012. Tectonic implications and seismicity triggering during the 2008 Baluchistan, Pakistan earthquake sequence. *Journal of Asian Earth Sciences* 45, 167–178. <https://doi.org/10.1016/j.jseaes.2011.10.003>
- Yaghmaei-Sabegh, S., Gholamreza, O-A. 2021. Estimating of the b -value based on the characteristic earthquake model. *Journal of Earthquake and Tsunami* 15 (3), 2150015. <https://doi.org/10.1142/S1793431121500159>

Internet sources:

AFAD, 2022. <https://tdth.afad.gov.tr> (Accessed February 04, 2022)

Active Fault Map of Turkey. General Directorate of Mineral Research and Explorations Special Publications Series, Ankara-Turkey. <http://www.mta.gov.tr/v3.0/hizmetler/yenilenmis-diri-fay-haritalari> (Accessed January 17, 2022)